AGU PUBLICATIONS

Water Resources Research

RESEARCH ARTICLE
10.1002/2013WR015044

Special Section:
Eco-hydrology of Semiarid Environments: Confronting Mathematical Models with Ecosystem Complexity

Interannual variability of evapotranspiration and vegetation productivity

Simone Fatichi[1] and Valeriy Y. Ivanov[1,2]

[1]Institute of Environmental Engineering, ETH Zurich, Zürich, Switzerland, [2]Department of Civil and Environmental Engineering, University of Michigan, Ann Arbor, Michigan, USA

Abstract Interannual variability of precipitation can influence components of the hydrological budget, affecting them directly and indirectly through adjustments in vegetation structure and function. We investigate the effects of fluctuations of annual precipitation on ecohydrological dynamics. Specifically, we use the advanced weather generator, AWE-GEN, to simulate 200 years of hourly meteorological forcing obtained by imposing four types of precipitation annual process with identical long-term mean. The generated time series force a mechanistic ecohydrological model, Tethys-Chloris. Simulations with perturbed precipitation variability are performed for four locations characterized by different vegetation cover and climate. The results indicate that long-term transpiration (T) and evapotranspiration (ET) fluxes as well as vegetation productivity expressed as Gross Primary Production (GPP) and Aboveground Net Primary Production (ANPP) are essentially unaffected by the imposed climate fluctuations. This finding supports the hypothesis of a relative insensitivity, except for water-limited environments, of interannual evapotranspiration and vegetation productivity to annual climatic fluctuations, which are mostly reflected in the fluxes of deep leakage and runoff. The occurrence of short periods of favorable meteorological conditions randomly taking place within the year was found to be a better explanatory variable for interannual variability of ET and ANPP than average annual or growing season conditions. The results indicated that local, single-site sensitivities are considerably smaller than those observed across climatic and vegetation spatial gradients and thus an important role of ecosystem reorganization in modifying ANPP and ET sensitivity in a changing climate is recognized.

Key Points:
- Sensitivities are larger for changes in precipitation mean than variance
- Sensitivities to changes in precipitation are larger regionally than locally
- Short temporal scales are controlling interannual variability of ET and ANPP

Supporting Information:
- Auxiliary material Info
- WRR_Supplementary_Material

Correspondence to:
S. Fatichi,
simone.fatichi@ifu.baug.ethz.ch

Citation:
Fatichi, S., and V. Y. Ivanov (2014), Interannual variability of evapotranspiration and vegetation productivity, *Water Resour. Res.*, *50*, 3275–3294, doi:10.1002/2013WR015044.

Received 12 NOV 2013
Accepted 23 MAR 2014
Accepted article online 28 MAR 2014
Published online 15 APR 2014

1. Introduction

Climatic fluctuations at different temporal scales, from hourly to multiannual, significantly affect energy, water, and carbon fluxes at the land surface [e.g., *Wilson and Baldocchi*, 2000; *Baldocchi*, 2008; *Urbanski et al*., 2007; *Bonan*, 2008]. In the range of temporal scales, the controls exerted by the interannual climate variability have been shown to provide rather different responses in terms of hydrological and vegetation dynamics. Previous studies have demonstrated responses ranging from a strong control of annual precipitation on carbon and water fluxes [*Williams and Albertson*, 2005; *Yang et al*., 2008] to insensitivity of annual transpiration and/or evapotranspiration to variability of annual precipitation [*Roberts*, 1983; *Phillips and Oren*, 2001; *Oishi et al*., 2010]. Mixed responses relative to vegetation type have been also found [*Holmgren et al*., 2013], even for similar climatic and soil conditions [*Stoy et al*., 2006]. As follows, these results do not always match an a priori expectation that with increasing aridity, the annual variability of precipitation should exert a progressively larger control on annual evapotranspiration and vegetation productivity [e.g., *Bréda et al*., 2006; *Koster and Suarez*, 1999]. Concurrently, the capability of plants to use available water in drier years or sites more efficiently was also reported [*Troch et al*., 2009; *Brooks et al*., 2011] and expressed through a negative correlation of the Horton index (the ratio between total evapotranspiration and precipitation minus fast runoff) with the humidity index (the ratio between precipitation and potential evapotranspiration).

In terms of carbon cycle, when global-scale, multisite relationships were analyzed, the Aboveground Net Primary Production (ANPP) was found to be significantly correlated with annual or growing season precipitation. However, a much lower sensitivity was observed locally, at the scale of a single site [*Sala et al*., 1988; *Lauenroth and Sala*, 1992; *Knapp and Smith*, 2001; *Huxman et al*., 2004; *Guo et al*., 2012; *Hsu et al*., 2012], with few exceptions [*Fang et al*., 2001].

Previous studies on hydrological and ecological response to annual climate variability have been generally limited by the short records of available data, the difficulties of designing manipulation experiments with

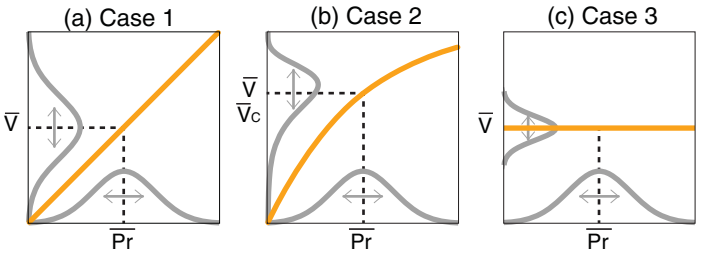

Figure 1. A conceptual diagram of possible responses of a dependent variable (such as ET or ANPP) with mean $\bar{V}$ to changes in the second-order moment properties of annual precipitation, where $\overline{Pr}$ is the mean annual precipitation. (a) If the relationship between the two variables is linear, a change in the precipitation variance does not affect the mean of the dependent variable but only the variance. (b) In the case when a nonlinear, concave down relationship exists, a change in the precipitation variance skews the distribution of the dependent variable such that the changed mean $\bar{V}_C$ will decrease relative to the present mean $\bar{V}$. Also affected is the variance of the dependent variable. (c) In the third case, when the two variables are independent neither the mean nor the variance of the dependent variable is affected by changes in the precipitation variance.

imposed interannual precipitation variability (but see *Knapp et al*. [2001] and *Collins et al*. [2012] for exceptions), and technical capabilities to measure quantities suitable for characterizing all relevant hydrological and ecological state variables. In order to overcome some of the above limitations and characterize the response of different ecosystems to changes in interannual variability of precipitation, we constructed a set of numerical experiments that are based on two advanced tools: an hourly weather generator, AWE-GEN [*Ivanov et al*., 2007; *Fatichi et al*., 2011], and a mechanistic ecohydrological model, Tethys-Chloris [*Fatichi et al*., 2012a, 2012b]. The weather generator is a stochastic simulator designed to produce hourly time series of weather variables for a given stationary climate. AWE-GEN is capable of reproducing statistical characteristics of meteorological variables across a wide range of temporal scales, from the high-frequency hourly values to the low-frequency interannual variability, a feature that is specifically crucial for this study. The mechanistic ecohydrological model, Tethys-Chloris, simulates all essential components of the hydrological cycle, resolving the mass and energy budgets at the hourly scale, and includes vegetation dynamics in an explicit prognostic framework, although longer time scale processes, such as species competition and forest successional dynamics, are not simulated.

The weather generator, AWE-GEN, is used to simulate several long-term scenarios of hourly climate time series, imposing different modes of interannual precipitation variability. Changes in interannual variability are obtained modifying the long memory of annual precipitation as well as its variance (as described later) for four locations characterized by different climates and dominant vegetation types. After having been tested for these locations, the ecohydrological model, Tethys-Chloris (T-C), is used to simulate energy, water, and carbon dynamics over the duration of the synthetic climate time series. The analysis of the designed scenarios identifies on the relative importance of climatic conditions at different temporal scales in controlling annual variability of evapotranspiration (ET) and vegetation productivity. Additionally, the analysis reveals how changes in interannual variability of precipitation affect a number of representative variables, following a conceptual scheme after *Jensen* [1906] and *Hsu et al*. [2012] (Figure 1). Three possible cases are identified as a consequence of a change in annual precipitation variability at the level of a vegetation stand. In the first case, the annual value of the dependent variable (e.g., ET or ANPP of the stand) with the mean $\bar{V}$ is linearly related to precipitation *Pr* (with the mean $\overline{Pr}$). Consequently, a change in the annual variability of *Pr* leads to a change in the variance of the dependent variable but not to a change in its mean. In the second case, a nonlinear relationship exists between the dependent variable and *Pr*; therefore, a change in the variance of *Pr* leads to a change in both the mean and the variance of the dependent variable. In the third case, the dependent variable is insensitive to *Pr*. As such, changes in the variance of *Pr* affect neither the mean $\bar{V}$, nor the variance of the dependent variable.

Using the designed numerical experiments, we address the following questions: (i) Are vegetation productivity (Gross Primary Production (GPP) and ANPP) and evapotranspiration sensitive to changes in the mean and variance of annual precipitation? (ii) If they are insensitive, what other time scales control the variability of annual ET, GPP, and ANPP, given a certain long-term climate?, (iii) Is there a role of precipitation long-term persistence (memory) in controlling annual ET, GPP, and ANPP?, (iv) Are there significant differences across a range of climates and vegetation types? Answering the above questions can help enhancing the understanding of sensitivity of ecosystems to climate variability. A possibly more important scope is to consider these questions in the context of climate change, which has the capacity to modify not only the long-term mean precipitation but also its interannual variability [e.g., *Rowell*, 2005].

2. Materials and Methods

2.1. Case Studies

Four locations characterized by different vegetation types and climatic conditions were used in the following numerical experiments. These are represented by a deciduous forest in the northern lower peninsula of Michigan (UMBS), a seasonally dry grassland in California (Vaira Ranch), a semiarid shrub ecosystem in the Walnut Gulch experimental watershed in south Arizona (Lucky-Hills), and a wet grassland in central Switzerland (Zürich). Since only a few ($<$10) years of meteorological data were available from the experimental sites, in two out of the four locations, the long-term climatic series from nearby meteorological stations were used to identify the parameters of the weather generator and thus to define the baseline climates for the subsequent numerical experiments.

2.1.1. The University of Michigan Biological Station (UMBS), MI, USA

The model T-C was confirmed using almost 12 years (January 1999 to October 2010) of eddy covariance flux measurements collected in a deciduous forest in the north of the lower Michigan peninsula, near the University of Michigan Biological Station, UMBS (84.71°W, 45.55°N; elevation 234 m a.s.l.). The dominant canopy species include *Populus grandidentata Michx.* (bigtooth aspen) and *Populus tremuloides Michx.* (trembling aspen), which together comprise over 40% of the basal area. The other species are *Quercus rubra L.* (northern red oak), *Betula papyrifera Marsh.* (paper birch), *Fagus grandifolia Ehrh.* (American beech), *Acer saccharum Marsh.* (sugar maple), *Acer rubrum L.* (red maple), and *Pinus strobus L.* (white pine). The understory vegetation primarily consists of bracken fern and saplings of the canopy species. The mean annual temperature and precipitation in the analyzed period are 7.1 °C and 873 mm, respectively. In combination with eddy covariance flux measurements, Leaf Area Index (LAI), soil temperature, and soil moisture have been also collected and were used for model confirmation. Annual estimates of fine root biomass, leaf litter, and aboveground biomass increments are also available. For a full description of the site and observation methodologies, the reader is referred to *Bovard et al.* [2005], *Curtis et al.* [2005], *Gough et al.* [2007, 2009, 2013], and *He et al.* [2013, 2014].

A column of soil 3 m deep is assumed in the simulation with a free drainage condition at the bottom; the root depth (defined as the depth which includes 95% of fine root biomass) is assumed to be 80 cm according to local observations [*He et al.*, 2013]. Soil hydraulic properties are also assigned based on local observations [*He et al.*, 2013].

2.1.2. Vaira Ranch—San Francisco, CA, USA

We used a data set corresponding to the flux tower near the Vaira Ranch (120.95°W, 38.41°N; elevation 129 m a.s.l.) located in the lower foothills of the Sierra Nevada Mountains, near Ione, California. The ecosystem is classified as a "California, annual grassland." The open grassland is dominated by C_3 annual species, including *Brachypodium distachyon L.*, *Hypochaeris glabra L.*, *Trifolium dubium Sibth.*, *Trifolium hirtum All.*, *Dichelostemma volubile A.*, and *Erodium botrys Cav.* [*Ma et al.*, 2007]. The climate at Vaira Ranch can be classified as Mediterranean type, with dry, hot summers and wet, mild winters. The long-term mean annual temperature and precipitation are 16.9 °C and 565 mm, respectively [*Ryu et al.*, 2008]. For a detailed description of the site including climate, soil, and vegetation characteristics, the reader is referred to *Baldocchi et al.* [2004], *Xu and Baldocchi* [2004], *Ma et al.* [2007], and *Ryu et al.* [2008]. T-C was tested for a period of nearly 9 years (November 2000 to December 2009). The simulation plot is considered to be flat and fully occupied by a C_3 grass. A soil column 1 m deep and a root depth of 30 cm were assumed in the simulation. Homogenous soil hydraulic properties were derived from pedotransfer functions using a 0.30 fraction of sand, 0.13 of clay, and 0.0139 of soil organic material.

Thirty years of hourly meteorological data from the station of San Francisco airport were used to calculate all of the parameters required by AWE-GEN. The location has a mean climate close to that characteristic of Vaira Ranch, with the mean annual temperature and precipitation of 13.3 °C and 538 mm, respectively.

2.1.3. Lucky Hills—Tucson, AZ, USA

The Lucky Hills experimental site (110.30°W, 31.44°N; elevation 1372 m a.s.l.) located within the Walnut Gulch Experimental Watershed, near Tombstone in the south-east Arizona, was used as a test case for T-C for a shrubland ecosystem. A flux tower has been measuring mass and energy exchanges since 1996 [*Emmerich and Verdugo*, 2008]. The flux tower footprint is composed of a sparse shrub community, mainly represented by evergreen shrubs, such as creosotebush (*Larrea tridentata*) and tarbush (*Flourensia cernua*),

and deciduous shrubs, such as whitethorn acacia (*Acacia constricta*) [*King et al*., 2008; *Skirvin et al*., 2008]. The mean annual temperature is 17.2 °C and the mean annual precipitation is ~333 mm [*Keefer et al*., 2008]. A more detailed description of site characteristics can be found in [*Fatichi et al*., 2012a, 2012b] and references therein. T-C was tested for a period of 13.5 years (July 1996 to December 2009). We considered a flat, plot-scale representation of surface composed of 0.25 fraction of whitethorn acacia and 0.10 fraction of creosotebush [*Weltz et al*., 1994]. A 2 m soil column depth is assumed in the simulations. The soil hydraulic properties are derived from pedotransfer functions, and the saturated hydraulic conductivity is assumed to decline exponentially with depth [*Fatichi et al*., 2012a]. A root depth of 90 cm was assumed on the basis of local observations [*Cox et al*., 1986].

2.1.4. Zürich, Switzerland

The performance of T-C for Swiss grasslands was tested using data from three flux tower sites located in a grassland region in the north-central part of Switzerland [*Fatichi et al*., 2014]. These are the experimental facilities of Chamau (47.21°N, 8.41°E; 393 m a.s.l.), Oensingen (47.28°N, 7.73°E; 452 m a.s.l.), and Früebüel (47.11°N, 8.53°E; 982 m a.s.l.). The data were available for several years, 2006–2008, 2002–2003, and 2006–2008, respectively. During the observational period, the three sites had annual precipitation totals of 1156, 1187, and 1690 mm yr^{-1} and average annual air temperatures of 9.6, 9.6, and 7.6 °C. A soil column of 1.5 m and a root depth of 25 cm were adopted for all of the locations. Soil properties were estimated from pedotransfer functions [*Fatichi et al*., 2014]. We consider a flat, plot-scale representation of surface fully covered by grassland, vegetation cover fraction $C_{crown}=1$. A full description of the locations with species composition can be found in *Ammann et al*. [2007, 2009], *Lazzarotto et al*. [2009], *Gilgen* [2009], *Gilgen and Buchmann* [2009], and *Zeeman et al*. [2010]. A detailed description of T-C simulations and model confirmation for these sites is reported in *Fatichi et al*. [2014].

Thirty years of hourly meteorological data from the station of Zürich, Fluntern were used to estimate the parameters of AWE-GEN. The station location corresponds to climate representative of the Swiss-plateau with the mean annual temperature and precipitation of 9.4 °C and 1126 mm, respectively.

2.2. Weather Generator and Experimental Design

AWE-GEN is a stochastic generator designed to produce hourly time series of weather variables for a given stationary climate and thus can produce theoretically infinitely long series. In situ, point-scale observations are required for estimation of its parameters [*Fatichi*, 2010; *Fatichi et al*., 2011, 2013]. The weather generator is capable of reproducing statistical characteristics of meteorological variables across a wide range of temporal scales, including interannual variability. Interannual dynamics are imposed by simulating annual precipitation through an autoregressive order-one model (AR1) or an autoregressive, fractionally integrated moving average (ARFIMA) model [*Montanari et al*., 1997; *Koutsoyiannis*, 2003; *Fatichi et al*., 2011]. The ARFIMA model is used to simulate the time series with long memory, i.e., where statistical dependence decays more slowly than an exponential decay, using a noninteger value of the long-memory (differencing) parameter d larger than zero [*Beran*, 1994]. The generator simulates seven meteorological variables: precipitation, cloudiness, air temperature, vapor pressure, wind speed, atmospheric pressure, and shortwave incoming radiation partitioned into diffuse and direct beam types and into two wavelength bands. AWE-GEN theoretical framework and parameter estimation can be found in *Fatichi et al*. [2011]. A technical reference of AWE-GEN is available online (http://www-personal.umich.edu/ivanov/HYDROWIT/Models.html).

For each of the selected locations, we stochastically generated 200-year long time series of hourly meteorological variables using the weather generator AWE-GEN. Four scenarios characterized by different interannual variabilities of precipitation were designed. We characterized the interannual variability of precipitation using five statistics of annual precipitation process: the mean $\overline{Pr}$, the coefficient of variation C_V, the skewness γ, the lag-1 correlation ρ_1, and the long-memory parameter d, which is related to the Hurst coefficient H_u, through $d=H_u-0.5$ [*Fatichi et al*., 2012c]. Their derived values for the four analyzed locations are presented in Table 1, along with other climatic information. Note that the precipitation statistics in Table 1 computed from long-term monthly time series are slightly different from the statistics of the hourly time series derived from the flux tower observations (section 2.1). The parameter d is not reported since its estimation for a single site is not robust, given the short duration of observed climate time series. However, a global-scale analysis points to a value of $d \approx 0.16$, which is significantly different from zero [*Fatichi et al*., 2012c].

Table 1. Site Characteristics as Inferred From Observed Data[a]

	UMBS	Vaira	Lucky Hills	Zürich
Number of years	31	155	49	30
$\overline{Pr}$ (mm yr^{-1})	814	539	354	1126
C_V (–)	0.14	0.30	0.24	0.15
γ (–)	−0.16	0.38	0.28	0.60
$\rho_1(-)$	0.007	0.075	0.293	0.081
T_a (°C)	7.9	13.3	17.2	9.4
R_{sw} (Wm^{-2})	157	182	236	128
R_n (Wm^{-2})	81	92	105	63
E_{pot} (mm yr^{-1})	1043	1185	1356	812
DI (–)	1.28	2.19	3.83	0.72

[a]The quantities $\overline{Pr}$ (mm yr^{-1}), C_V (–), γ (–), and $\rho_1(-)$ are the mean, coefficient of variation, skewness, and lag-1 autocorrelation of annual precipitation, respectively. Other site variables are long-term averages of air temperature T_a (°C), shortwave radiation R_{sw} (W m^{-2}), net radiation R_n, potential evaporation (computed from Penman-Monteith equation as in *Shuttleworth* [1993]) E_{pot} (mm yr^{-1}), and the dryness index $DI = E_{pot}/\overline{Pr}(-)$.

The four selected scenarios of interannual variability are represented by (i) a reference scenario, in which annual precipitation is simulated with an AR1 model, with the skewness modified through the Wilson-Hilferty transformation (AR case); (ii) a scenario in which annual precipitation is simulated with an ARFIMA model with $d = 0.35$, which intentionally exaggerates the natural long memory of the time series (ARFIMA case); (iii) a scenario in which the annual precipitation is simulated with an AR1 model but the variance of annual precipitation is changed with respect to the reference scenario, so as to increase the coefficient of variation C_V by $+0.1$ (ARp01 case); and (iv) a scenario in which annual precipitation is also simulated with an AR1 model but the coefficient of variation C_V is decreased by 0.1, with respect to the reference scenario, changing again the variance of the process (ARm01 case). These four scenarios, the reference (AR), the long memory (ARFIMA), the increased (ARp01), and the decreased (ARm01) precipitation interannual variability permit testing the response of ecohydrological system to changes in interannual variability, since in all of the scenarios the long-term mean precipitation is the same. Note that the applied changes in C_V of ± 0.1 should be considered as a rather drastic modification, with the typical worldwide range of C_V corresponding to 0.15–0.5 [*Fatichi et al*., 2012c; *D'Odorico and Bhattachan*, 2012]. Imposing such a large change in C_V, as well as a strong intensity of the long memory, has the objective of amplifying the simulated responses of the studied ecosystems.

Further, note that while the annual perturbation scenarios target only the process of precipitation, due to the causal and statistical linkages of precipitation with most of the other meteorological variables simulated by AWE-GEN [*Fatichi et al*., 2011, 2013], we expect that the latter variables will exhibit fluctuations consistent with that of precipitation.

The 200 years of generated hourly meteorological variables for the four scenarios of interannual variability are used as input to the ecohydrological model T-C.

2.3. Ecohydrological Model

The mechanistic ecohydrological model, Tethys-Chloris (T-C), simulates all essential components of the hydrological cycle, resolving the mass and energy budgets at the hourly scale. It includes energy and mass exchanges in the surface boundary layer, using a detailed resistance analogy scheme [e.g., *Sellers et al*., 1997], a module of saturated and unsaturated soil water dynamics, up to two layers of vegetation, and a snowpack evolution module. The dynamics of water content in the soil profile are resolved using the one-dimensional (1-D) Richards equation for vertical flow and the kinematic wave formulation for lateral subsurface flow. Vegetation dynamics are represented and include all essential plant life-cycle processes, i.e., photosynthesis, phenology, carbon allocation and translocation, and tissue turnover [*Fatichi et al*., 2012a, 2012b]. The version of T-C used in this study includes modifications introduced in *Fatichi and Leuzinger* [2013] and *Fatichi et al*. [2014]. Specifically, the soil heat flux is computed solving the heat diffusion equation, water ponding on surface is included as an option, "two big-leaves" scheme is introduced, where sunlit and shaded leaves are treated separately for computing net assimilation and stomatal resistance, standing dead biomass and fruit-flower carbon pools are explicitly simulated, and, lastly, grassland management

practices (grazing, cutting) can be also represented by the model. A detailed description of the model is provided in *Fatichi* [2010] and *Fatichi et al*. [2012a, 2012b].

While the model can resolve ecohydrological dynamics over complex topography of a watershed and explicitly consider spatial variability of meteorological fields and the role of topography in controlling incoming radiation and water lateral transfers, in this study, each domain was assumed to be flat without lateral effects of mass and energy exchange and without an explicit areal dimension. All computed one-dimensional fluxes and storages are obtained per unit ground area.

Vegetation in T-C is dynamic as all of the simulated carbon pools evolve in time, responding to climatic inputs and boundary conditions. However, the model assumes vegetation in a mature state, without simulating further ecosystem processes such as forest growth, species competition and successional dynamics. Vegetation also does not age, seeds are not dispersed, and recruitment does not occur. Mortality events can occur only because of carbon starvation, when mobile nonstructural carbohydrate reserves are entirely depleted (no mortality episodes were observed in the presented simulations). Therefore, persistent effects of severe droughts on forest composition and structure due to mortality caused by hydraulic failure or biotic agents cannot be accounted for. Nutrient dynamics are also neglected in the model that assumes vegetation to be in equilibrium with its nutritional environment.

The above assumptions are certainly critical for analyzing long-term energy, water, and carbon fluxes. However, mechanistic modeling of processes such as seed dispersal, recruitment, forest successional dynamics, or plant mortality is particularly challenging. Due to the current lack of commonly accepted approaches, their representations would require numerous assumptions and parameterizations that would remain untested using only flux tower data, and difficult to test even with forest inventories or remote sensing data [*Medlyn et al*., 2005]. Similar issues impact a numerical representation of nutrient dynamics. Therefore, the design of this study had a specific focus on the investigation of responses of "established ecosystems" to annual variability of precipitation. We omit the effects of transient processes of forest demography, nutrient controls, and the impacts of abrupt changes due to mortality in extreme years from our simulations. The implications of these limiting assumptions are further discussed in section 4.

2.4. Sensitivities and Indexes

In order to analyze the effect of perturbing the annual precipitation process on ET, GPP, and ANPP, we compute "normalized sensitivities" to mean annual precipitation and to the second-order moment property of precipitation process. In the former case, the sensitivity is computed for each of the four interannual variability scenarios; a single sensitivity is estimated in the latter case, using the difference between the long-term means of variables of interest in the scenarios ARp01 and ARm01.

Specifically, the normalized sensitivity to mean annual precipitation $S_{\mu,\mu}$ is computed from the slope β of the linear relationship (the linear least squares fit) between a prognostic variable at the annual scale V (e.g., ET, GPP, or ANPP) and annual precipitation Pr multiplied by the ratio of mean precipitation $\overline{Pr}$ to the mean of V, $\bar{V}$, $S_{\mu,\mu}=\beta\cdot\overline{Pr}/\bar{V}$ [*Hsu et al*., 2012]. The normalized sensitivity to the second-order moment property of annual precipitation $S_{\mu,\sigma}$ is computed as $S_{\mu,\sigma}=\Delta\bar{V}/\Delta\sigma_{Pr}\cdot\overline{\sigma_{Pr}}/\overline{V_{pm}}$, where $\Delta\bar{V}$ and $\Delta\sigma_{Pr}$ are the differences of the means $\bar{V}$ and of the standard deviations σ_{Pr} of annual precipitation corresponding to the ARp01 and ARm01 scenarios. The variables $\overline{V_{pm}}$ and $\overline{\sigma_{Pr}}$ are the means of the two values obtained for the ARp01 and ARm01 scenarios. Finally, the sensitivity of a second-order moment property of a variable V to the second-order moment property of annual precipitation is computed as $S_{\sigma,\sigma}=\Delta\sigma_V/\Delta\sigma_{Pr}\cdot\overline{\sigma_{Pr}}/\overline{\sigma_V}$, where, as above, the differences and the means of σ_V and σ_{Pr} are computed using the values obtained for the ARp01 and ARm01 scenarios. The normalized sensitivities are useful metrics because they conveniently express the magnitude of a relative expected change in one variable, given a relative change in the other. For instance, $S_{\mu,\mu}=1$ implies that a change of 1% in the precipitation mean leads to a 1% change in the mean of the dependent variable V (e.g., ET).

Additionally, we compute an index that expresses a combination of climatic and vegetation controls during the growing season. Specifically, *Stoy et al*. [2006] identified a growing season index GS_p, computed as the product of four variables representing the growing season: precipitation (integrated), vapor pressure deficit, stomatal conductance, and Leaf Area Index (all averaged). This index was found to provide a good explanatory power for growing season and annual variability of evapotranspiration.

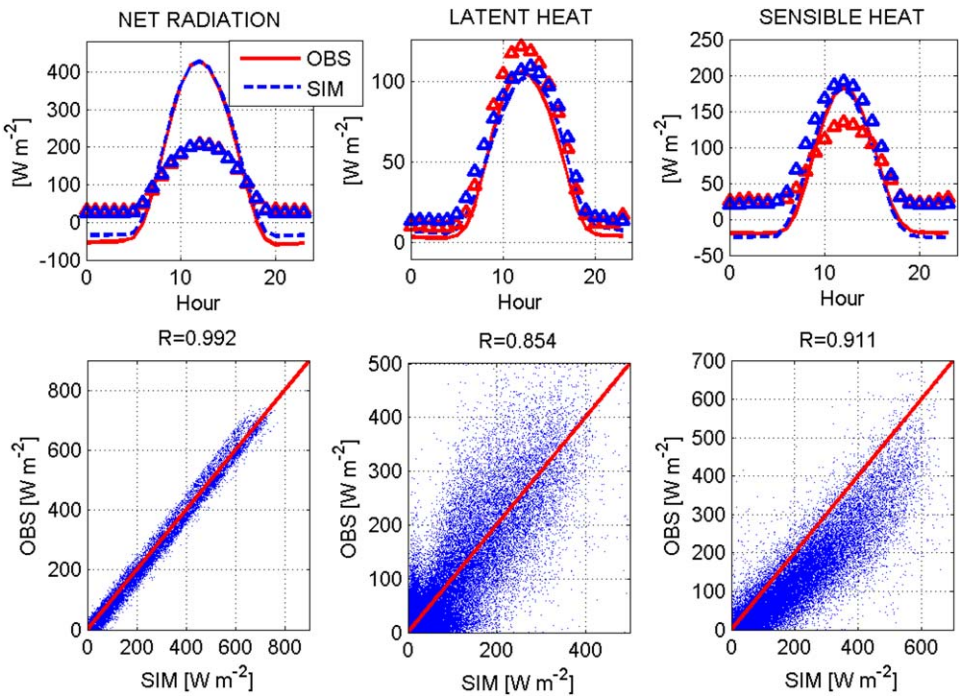

Figure 2. A comparison between the observed (OBS) and simulated (SIM) average daily cycles of net radiation, latent heat, and sensible heat for the location of the UMBS. The triangles represent the standard deviations. The scatterplots with correlation coefficients *R* are shown for observations at the hourly scale.

Finally, in this study we define two metrics "good days," *GD*, and "good hours," *GH*, as the number of days and hours within a year, where the simulated ET is larger than the 95th percentile of the simulated daily or hourly ET in the observational period. Such metrics are intended to capture hours/days where a combination of favorable temperature, fully developed canopy, high soil moisture, favorable vapor pressure deficit, and wind speed conditions lead to very high magnitudes of ET (and, supposedly, GPP). The choice of the 95th percentile is arbitrary but it affects the results only marginally, and similar results are obtained using the 85th and 90th percentiles, as discussed in the following.

3. Results

3.1. Model Confirmation

In this section, we present confirmation of T-C performance only for the locations of the UMBS and Vaira Ranch. We compare multiyear hourly simulations of energy, water, and carbon fluxes with detailed measurements available for the respective flux towers. The T-C simulation for the location of Lucky Hills is described in *Fatichi et al*. [2012a]. Simulations for three flux towers representative of grassland in Switzerland are described in *Fatichi et al*. [2014]. They all show satisfactory results. The updated version of T-C, especially the two big-leaves parameterization, allows us to obtain even better results for long-term carbon fluxes at Lucky Hills, as compared to *Fatichi et al*. [2012a]. This improved performance is reported in the supporting information (Figure S1).

3.1.1. UMBS

The mean daily cycles of energy fluxes at the UMBS are reproduced with a high degree of accuracy by T-C as testified by the determination coefficients R^2 for the entire simulation period: $R^2=0.98$ for net radiation R_n, $R^2=0.83$ for sensible heat H, and $R^2=0.73$ for latent heat λE, computed at the hourly scale (Figure 2). Latent heat is overestimated by 9.2% by the model, when compared to the flux tower data. However, the energy budget is closed only in the model simulations and is not satisfied in the flux data. This result is supported by previous studies showing that nonclosure of the energy budget at UMBS is mainly attributed to an underestimation of latent heat in the flux tower measurements [*Schmid et al*., 2000; *Su et al*., 2004].

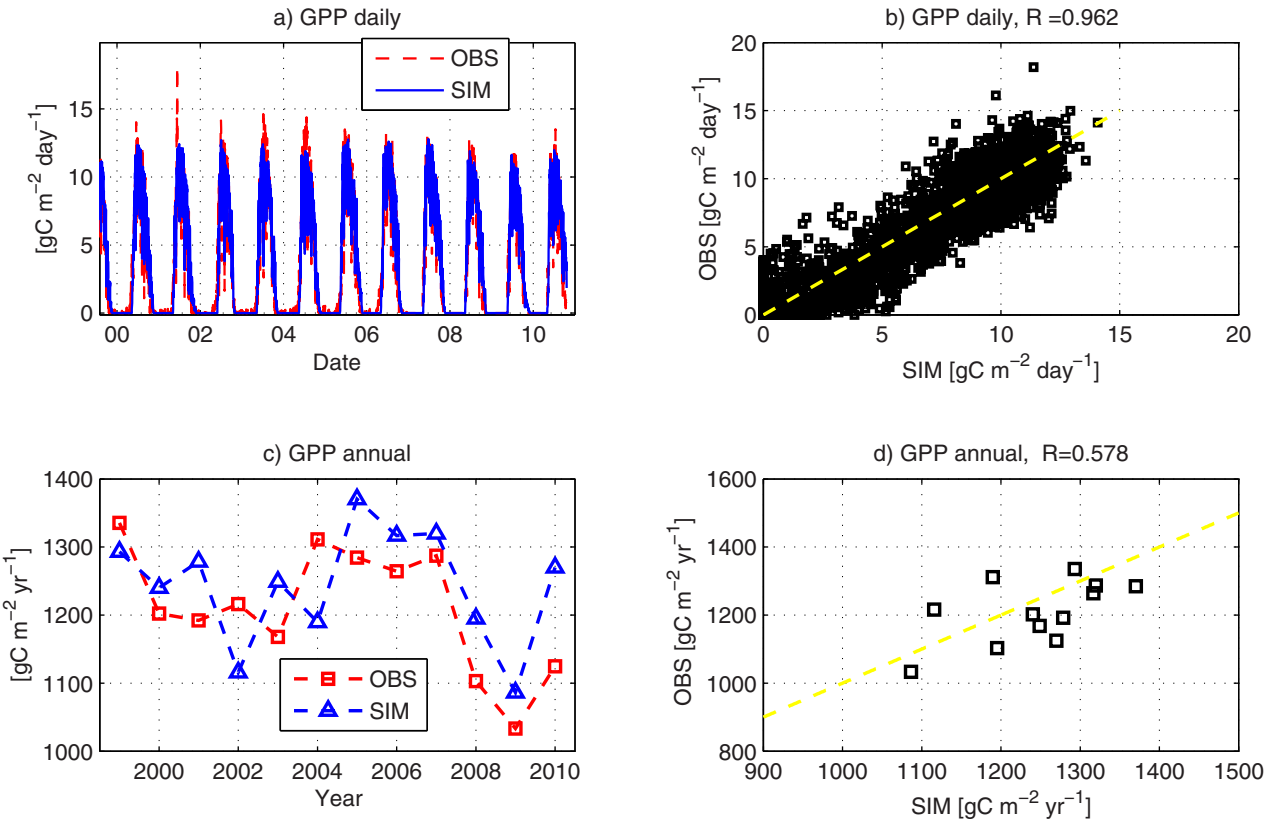

Figure 3. A comparison between the observed (OBS) and simulated (SIM) (a) daily and (c) annual GPP for the location of the UMBS. The scatterplots with the correlation coefficients *R* are shown for (b) daily and (d) annual GPP.

The temporal dynamics of soil moisture are compared to observations at various depths for a monitoring period of less than 2 years, 2009–2010 (supporting information, Figure S2). The model is capable of simulating well soil moisture dynamics at 5, 15, 30, and 60 cm depth, with small underestimation (30 cm) or overestimation (15 cm). Model performance of soil moisture dynamics at 100 and 200 cm is considerably lower, where the simulated range of variability overestimates observations. At 200 cm, the model also systematically predicts larger soil moisture contents, while the simulated λE is also larger.

The simulated GPP at the daily time scale is compared to GPP calculated from the observed Net Ecosystem Exchange (NEE, the net exchange of carbon fluxes in the vertical direction) and estimated ecosystem respiration (Figure 3). The results show a very good match in terms of temporal dynamics ($R^2=0.92$), testifying appropriate simulation of site phenology and intra-annual variability (not discernible in the figure). The total annual GPP from simulations and that derived from observations are 1243 and 1210 gC m^{-2} ground yr^{-1}, respectively. Despite such a good result at the daily scale, the performance in reproducing the annual GPP is inferior with $R^2=0.33$. Note that given the relatively small standard deviation of the annual GPP at the UMBS 91 gC m^{-2} ground yr^{-1}, it is difficult to verify how much of the model versus data difference in annual values can be attributed to a model deficiency and how much can be related to uncertainties in annual flux tower estimates.

Finally, the ground observations of Leaf Area Index (LAI) are compared with T-C simulations (supporting information, Figure S3). The model exhibits the capability to capture the phenology of leaf onset quite well, although 5–7 days of delay in model simulations can be detected. The same applies to the timing of leaf senescence. Summer peaks of LAI are well reproduced with small differences detectable in the first 3 years of the simulation. Remote sensing products, i.e., Moderate Resolution Imaging Spectroradiometer (MODIS) data, give considerably higher peaks of LAI with respect to the ground observations (not shown).

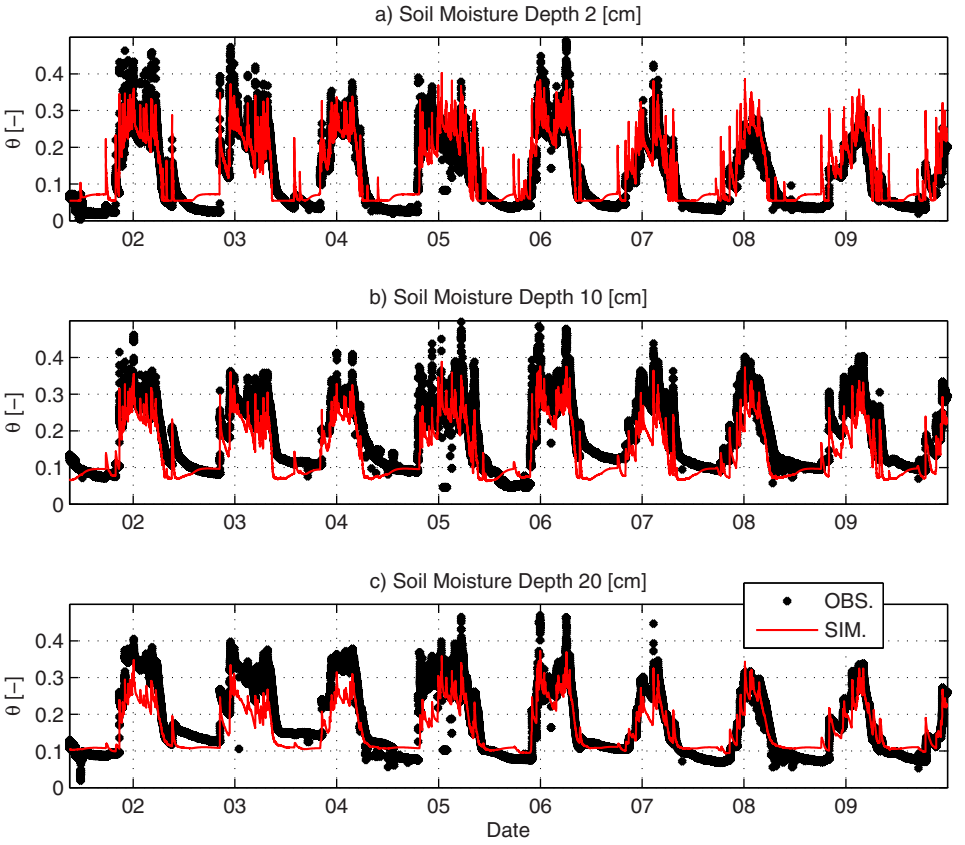

Figure 4. A comparison between the observed (OBS) and simulated (SIM) soil water content at different depths: (a) 2 cm, (b) 10 cm, and (c) 20 cm, measured near the Vaira Ranch flux tower.

3.1.2. Vaira Ranch

The model also satisfactorily reproduces the mean daily cycles of net radiation R_n, sensible heat H, and latent heat λE, and their corresponding standard deviations for the location of Vaira Ranch (supporting information, Figure S4). Non-negligible overestimation of R_n and H can be appreciated during midday hours. The mismatch is mainly limited to the period from March through June and can be the result of two combined effects: an underestimation of the surface albedo and a misrepresentation of the surface temperature. The determination coefficients for the entire simulation computed at the hourly scale are $R^2=0.96$ for R_n, $R^2=0.88$ for H, $R^2=0.71$ for λE, and $R^2=0.72$ for ground heat flux G. The model thus explains most of the variability in the hourly energy fluxes during the 9 years of the simulation.

The simulated time series of soil moisture at three depths are compared with the observations in Figure 4. T-C captures the dynamics of soil moisture and reproduces the dissipation of soil moisture pulses quite well at different time scales. The determination coefficients computed at the hourly scale are high ($R^2=0.78$ at 2 cm depth, $R^2=0.76$ at 10 cm depth, and $R^2=0.77$ at a depth of 20 cm) and comparable among the three depths. The Root Mean Square Error (RMSE) of hourly soil moisture is also similar across the three depths and in the range of 0.043–0.057 (–). This underlines the consistency of the model performance for deeper layers and a substantial reliability of the pedotransfer function used to estimate the soil hydraulic properties.

The time series of simulated daily GPP are similar to that calculated from the observed Net Ecosystem Exchange (NEE) and estimated ecosystem respiration (Figure 5a). The coefficient of determination at the daily scale is $R^2=0.71$ showing that more than two thirds of the variability in daily GPP is captured by the model. Annual GPP is evaluated by integrating fluxes over hydrological years (November to October) instead of calendar years [*Ma et al.*, 2007]. The T-C simulated average annual GPP of 810 gC m^{-2} ground

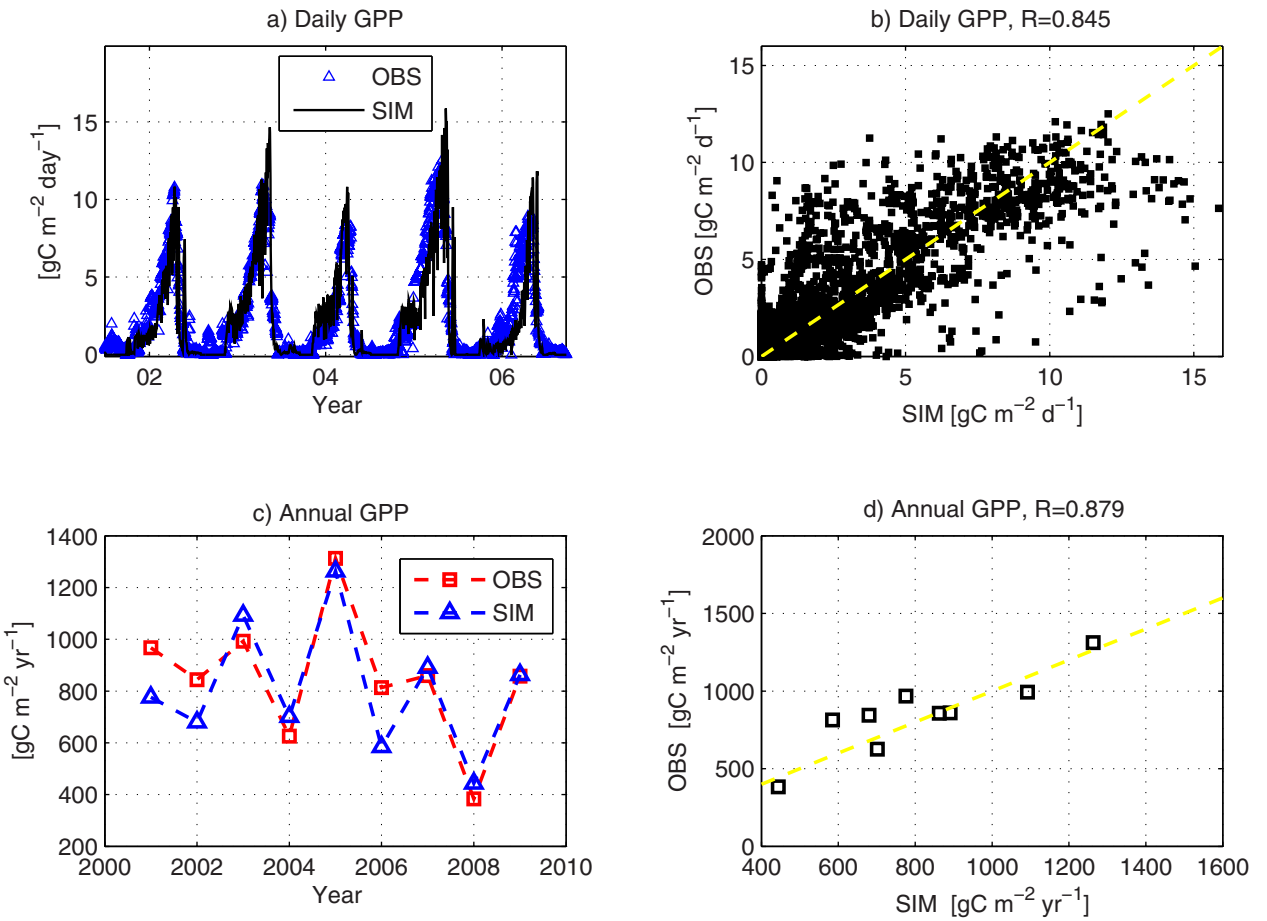

Figure 5. A comparison between the observed (OBS) and simulated (SIM) (a) daily and (c) annual GPP for the location of Vaira Ranch. The scatterplots with the correlation coefficients *R* are shown for (b) daily and (d) annual GPP.

yr^{-1} compares favorably with the value obtained from observations (NEE and ecosystem respiration) of 850 gC m^{-2} ground yr^{-1} (Figure 5b). The determination coefficient between the simulated and estimated annual GPP is relatively high, $R^2 = 0.77$ demonstrating that the model is capable of capturing the integrated annual effect of climate on vegetation production.

A comparison between the simulated versus ground-inferred and remotely inferred Leaf Area Index (LAI) illustrates that the model preserves the main features of the annual cycle of LAI and reproduces the annual peaks well (supporting information, Figure S5). There is however a seasonal delay in the aboveground biomass growth in the simulated time series, as compared to both ground observations and remote sensing estimates. Note that the remote sensing observations show an enduring leaf cover late in the growing season not supported by the ground observations. Model simulations support the presence of dead standing grass during late summer and fall, which probably leads to a reflectance typical of low LAI.

3.2. Results of Interannual Variability Scenarios

The imposed interannual variability scenarios ARp01 and ARm01 result in a substantial modification of the variance of annual precipitation that can be appreciated from a boxplot representation (Figure 6). The impact of introducing a long-term persistence scenario, i.e., the ARFIMA case, is not apparent in this representation for precipitation but expected to be appreciable through changes in other statistics. As seen, the variability in annual precipitation does not lead to any strongly pronounced effects in properties of several ecohydrological metrics, such as GPP, ET, and transpiration T, for at least three of the four locations (UMBS, Vaira Ranch, and Zürich). Transpiration is the metric most insensitive to the imposed precipitation scenarios: the mean, the variance, and the interquartile range are almost identical, regardless of the interannual

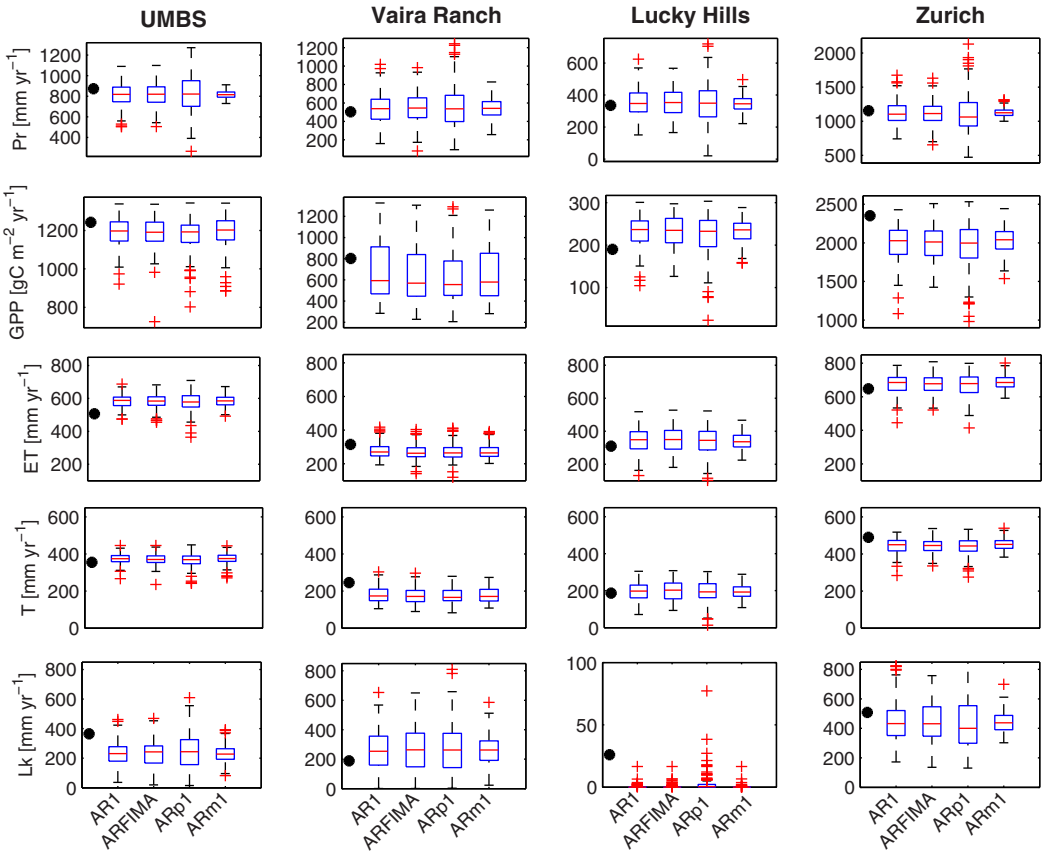

Figure 6. Boxplot representation of interannual variation of precipitation (Pr), Gross Primary Production (GPP), evapotranspiration (ET), transpiration (T), and deep leakage (Lk) for the four study locations and for the four scenarios of interannual variability: AR1, ARFIMA, ARp01, and ARm01. The black dot on the left of each plot represents the long-term mean from the observations (Pr) or simulations (GPP, ET, T, and Lk) during the observational periods. Note that for Vaira Ranch and Zürich hydrometeorological data of nearby meteorological stations with long-term data were used for generation of 200 years of hourly time series. Hydrometeorological data observed at the flux tower were used for simulations during the observational periods.

variability scenario. Only for the location of Lucky Hills, the interannual variability of precipitation, especially the ARp01 and ARm01 cases, leaves a signature in the ET and GPP statistics. For all of the other locations, the variability in precipitation is mostly translated into the variability of deep leakage (Lk), suggesting a general insensitivity of annual ET fluxes to the annual climate variability.

In order to explore this effect further, we analyzed the normalized sensitivities of ET, GPP, and ANPP (section 2.4). The results of normalized sensitivities for ET, GPP, and ANPP for all of the cases are reported in Table 2. Normalized sensitivities to the mean, $S_{\mu,\mu}$ for ET, GPP, and ANPP are always smaller than 1 and typically smaller than 0.5. Sensitivities are larger for the location of Lucky Hills, which is the driest location. The obtained values of $S_{\mu,\mu}$ are larger for ET than for ANPP or GPP, testifying that coupling of ET with precipitation is stronger than that for vegetation productivity. For instance, Vaira Ranch and the UMBS exhibit $S_{\mu,\mu}$ almost equal to zero for GPP and ANPP. The magnitudes of $S_{\mu,\mu}$ for ANPP are generally larger than for GPP, with the exception of the Vaira Ranch, testifying a response of the carbon allocation component to changes in precipitation.

The scenarios of interannual variability impact $S_{\mu,\mu}$ mostly for the sites of Lucky Hills and Zürich, as also shown by the larger sensitivities of the variance to change in the precipitation variance $S_{\sigma,\sigma}$. The normalized sensitivities of the mean to the variance $S_{\mu,\sigma}$ are always negative (case II in the conceptual model of Figure 1), but their absolute values are typically 20–40 times smaller than $S_{\mu,\mu}$. This behavior is similar to the conceptual case I (Figure 1) for Lucky Hills, and case III for the Vaira Ranch and the UMBS. A mix of the cases I and III appears to reflect the response characteristics of Zürich. The sensitivities of the variance of

Table 2. The Normalized Sensitivities $S_{\mu,\mu}$ of Annual Evapotranspiration (ET), Transpiration (T), Aboveground Net Primary Production (ANPP), and Gross Primary Production (GPP) to Changes in Annual Precipitation for the Four Interannual Variability Scenarios, Normalized Sensitivities $S_{\mu,\sigma}$ of Changes in Means of the Above Variables to Changes in Annual Precipitation Standard Deviation, and Normalized Sensitivities $S_{\sigma,\sigma}$ of Changes in Annual Standard Deviation of the Above Variables to Changes in the Annual Standard Deviation of Precipitation

		$S_{\mu,\mu}$					
Normalized Sensitivity		AR1	ARFIMA	ARp01	ARm01	$S_{\mu,\sigma}$	$S_{\sigma,\sigma}$
UMBS	ET	0.292	0.314	0.333	0.422	−0.010	0.308
	T	0.110	0.101	0.181	0.196	−0.016	0.113
	ANPP	0.083	0.043	0.156	0.087	−0.011	0.160
	GPP	0.047	0.021	0.109	0.049	−0.009	0.006
Vaira Ranch	ET	0.183	0.188	0.235	0.209	−0.024	0.132
	T	0.062	0.041	0.130	0.066	−0.015	−0.071
	ANPP	−0.062	−0.092	0.065	−0.105	0.000	−0.058
	GPP	0.063	0.004	0.142	0.092	−0.008	−0.066
Lucky Hills	ET	0.764	0.822	0.667	0.711	−0.006	0.722
	T	0.771	0.866	0.629	0.784	0.000	0.515
	ANPP	0.613	0.684	0.541	0.504	−0.044	0.627
	GPP	0.491	0.549	0.441	0.407	−0.039	0.638
Zürich	ET	0.336	0.332	0.280	0.231	−0.022	0.420
	T	0.268	0.249	0.221	0.173	−0.023	0.338
	ANPP	0.496	0.505	0.407	0.291	−0.037	0.412
	GPP	0.451	0.435	0.374	0.294	−0.025	0418

ET, GPP, and ANPP to changes in precipitation variance $S_{\sigma,\sigma}$ have a magnitude comparable to $S_{\mu,\mu}$ for all of the locations.

As seen in Figure 6, imposing a long-term memory (the ARFIMA scenario) has minimal effects on the annual fluxes. This result is largely confirmed by analyzing the autocorrelation functions of GPP and ET, which exhibit filtering of the strong correlation in annual precipitation (Figure 7). The autocorrelation structure is

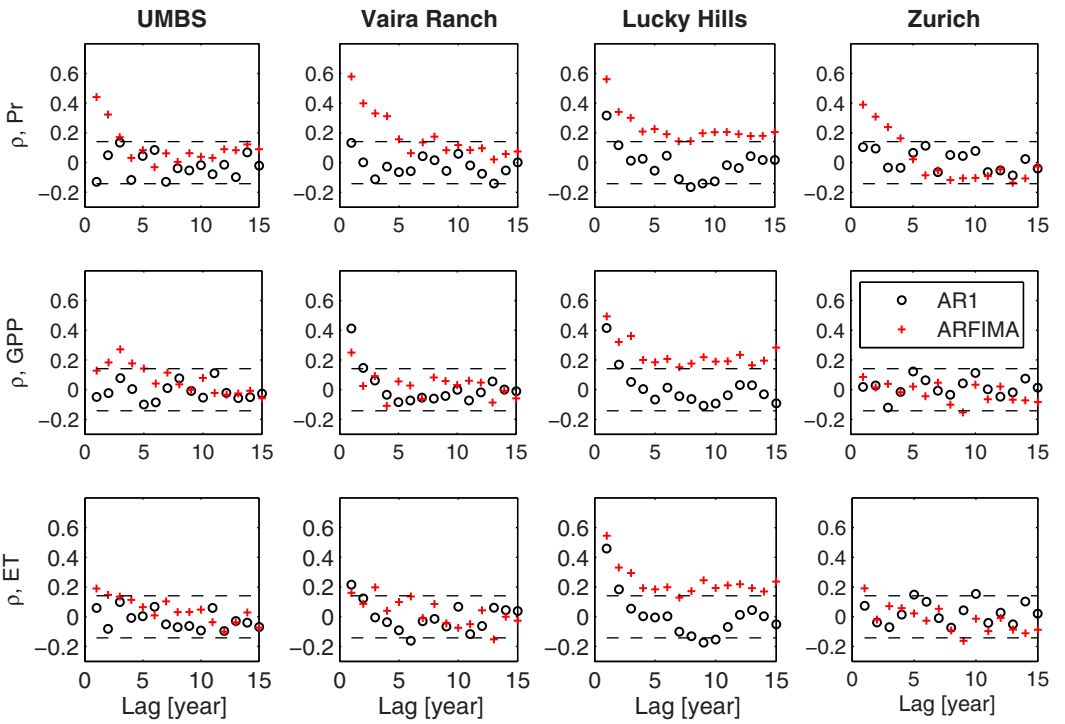

Figure 7. Sample autocorrelation functions of precipitation (Pr), Gross Primary Production (GPP), and evapotranspiration (ET) for the four analyzed locations and two scenarios of interannual variability: AR1 and ARFIMA. The upper and lower confidence bounds computed assuming that the series are Gaussian white noise, indicated by the dashed lines.

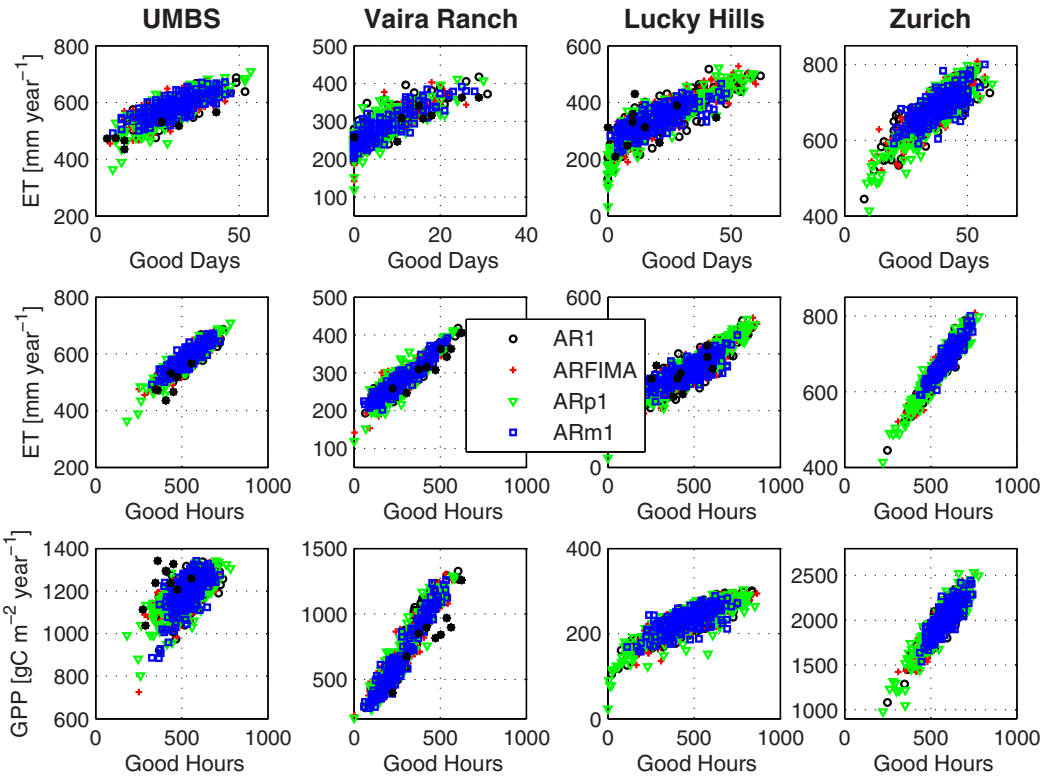

Figure 8. Scatterplots between the number of "good days" or "good hours" and the total annual evapotranspiration (ET) or Gross Primary Production (GPP) for the four analyzed locations. The different symbols and colors correspond to the four scenarios of interannual variability of precipitation. "Good days" ("good hours") are computed as the number of days (hours) within a year where the simulated ET is larger than the 95th percentile of the simulated daily (hourly) ET in the observational period. Values estimated from the same analysis of the flux tower observations are reported when available (the black filled circles).

preserved in ET and GPP only for the location of Lucky Hills. It can be also seen that annual GPP and ET for Vaira Ranch show a significantly positive lag-1 correlation for the reference scenario AR1, even in the absence of correlation in annual precipitation. Such a correlation is induced by memory in the belowground carbon pools of vegetation, which is an important component of the functioning of such a Mediterranean seasonal ecosystem.

The relative insensitivity of annual GPP and ET to annual precipitation variability demands for additional explanations on the controls underlying the year-to-year variability of these variables and points to the need of investigation at the intra-annual scales. We analyzed multiple linear and nonlinear correlations among meteorological and vegetation variables computed for different months and at the growing season scale to identify best possible statistical predictors of annual ET and GPP variability. As a result, the predictor proposed by *Stoy et al.* [2006], the growing season index GS_p, showed among the highest predictor skill for all the scenarios and locations. The growing season index was able to explain between 0.63 and 0.87 of growing season ET variability, depending on the location and case. Such a good (but not extraordinary) result further pointed to a role played by the higher-frequency dynamics occurring at temporal scales in the order of few days or even hours in explaining the interannual variability of ET and GPP.

We therefore hypothesized that a random occurrence of favorable conditions defined here as "good days," *GD*, and "good hours," *GH* (section 2.4), within a year could be a more suitable explanatory metric of annual ET and GPP than average conditions over a month, a growing season, or the entire year. Both the empirical data and the simulation results support this assertion (Figure 8), even though the short record available and gaps hamper the possibility of robust statistical inferences based only on flux tower data. The random occurrence of these favorable intervals within a year appears to exert a strong control on the interannual variability of, at the least, ET flux. The explanatory power is considerably higher than that for the growing season index GS_p or of growing season and annual precipitation. This is also demonstrated using boxplots

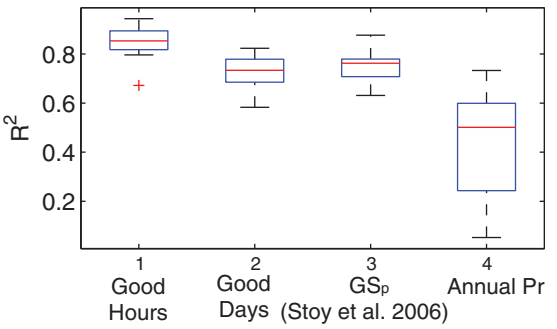

Figure 9. Boxplots representing the coefficients of determination between the annual evapotranspiration ET_{yr} and (1) "good hours," (2) "good days," (3) coefficients of determination between growing season evapotranspiration ET_{GS} and the growing season index, GS_p, as computed by *Stoy et al.* [2006], and (4) coefficients of determination between ET_{yr} and annual precipitation (Pr). Each boxplot represents 16 coefficients of determination corresponding to the four analyzed locations times the four scenarios of interannual variability, AR1, ARFIMA, ARp01, and ARm01.

of the determination coefficients between the annual or growing season ET and the different explanatory variables for the sixteen cases (four interannual variability scenarios per four locations) in Figure 9. The annual contribution of good days and good hours to the total annual ET ranges from 6–30% for *GD* to 26–41% for *GH*, underlining that fluxes occurring over just 5% of the year time can contribute more than one third of annual ET. The numbers of *GH* and *GD* have been found to be uncorrelated to the annual average energy forcing expressed both as shortwave radiation and net radiation.

4. Discussion

4.1. Sensitivity of Local-Scale Water and Carbon Fluxes

This study supports the hypothesis of a general insensitivity of the long-term, local-scale ET and vegetation productivity to precipitation interannual variability [*Knapp and Smith*, 2001; *Huxman et al*., 2004; *Hsu et al*., 2012; *Oishi et al*., 2010]. Sensitivities of the simulated means to a change in annual precipitation variance $S_{\mu,\sigma}$ are 20–40 times smaller than the sensitivities to changes in mean precipitation $S_{\mu,\mu}$. Concurrently, sensitivities of variance of ET and vegetation productivity to precipitation variance $S_{\sigma,\sigma}$ are comparable to $S_{\mu,\mu}$ but considerably smaller than 1. These sensitivities are representative for established mature ecosystems and for specific locations at the "stand scale"; therefore, they cannot be extended in space along energy and water availability gradients as discussed below.

As far as vegetation productivity is concerned, the most xeric location, Lucky Hills, and, partially, the wet grassland of Zürich exhibit a behavior that is more similar to the conceptual case I of Figure 1, with small sensitivities to mean precipitation and a relative insensitivity to changes in the variance. The case studies of the UMBS and Vaira Ranch show a behavior similar to the conceptual case III, with a substantial lack of sensitivity of GPP and ANPP to changes in annual precipitation mean and variance. The somehow surprising sensitivity of ANPP to precipitation in the wet climate of Zürich is mostly related to the scenario with increased interannual variability ARp01, which creates conditions for the occurrence of repeated dry periods during summer (the wettest season in Zürich). These unusual periods decrease the productivity of the short rooted grassland and therefore its annual ANPP. Note however that the sensitivities of vegetation productivity to precipitation are obtained without imposing any nutrient limitation effect on the ecosystem functioning. In relatively wet and nutrient-poor ecosystems, GPP and ANPP are expected to be even less sensitive to precipitation variability because nutrient limitation [*Oren et al*., 2001] tends to accentuate the nonlinearity of relationship between carbon uptake and transpiration.

The normalized sensitivity $S_{\mu,\mu}$ of ET is generally higher than for vegetation productivity but still much smaller than unity, pointing to a combination of the conceptual cases I and III in Figure 1. Climate fluctuations are mostly filtered by vegetation-related processes, which results in rather conservative ranges of annual ET and T (Figure 6). The coefficients of variation of annual ET and T are indeed smaller than the coefficients of variation of annual precipitation in all of the cases but ARm01. In this latter case, ET and T preserve the coefficients of variation of the base scenario AR1, which are larger than the coefficient of variation of annual precipitation in the ARm01 case. This underlines that ET and T annual variations are not necessarily always smaller than variability of precipitation (vegetation filters variability) but can be larger in particular conditions (vegetation enhances variability). The most logical explanation of this observation is that changes in precipitation interannual variability do not significantly affect the random occurrence of meteorological conditions conducive to high ET flux (i.e., "good hours"). This applies to nonlimiting conditions in terms of soil water. The frequency distribution of "good hours" is affected when soil control on vapor flux becomes progressively pronounced. This was demonstrated for the driest location, the Lucky Hills site.

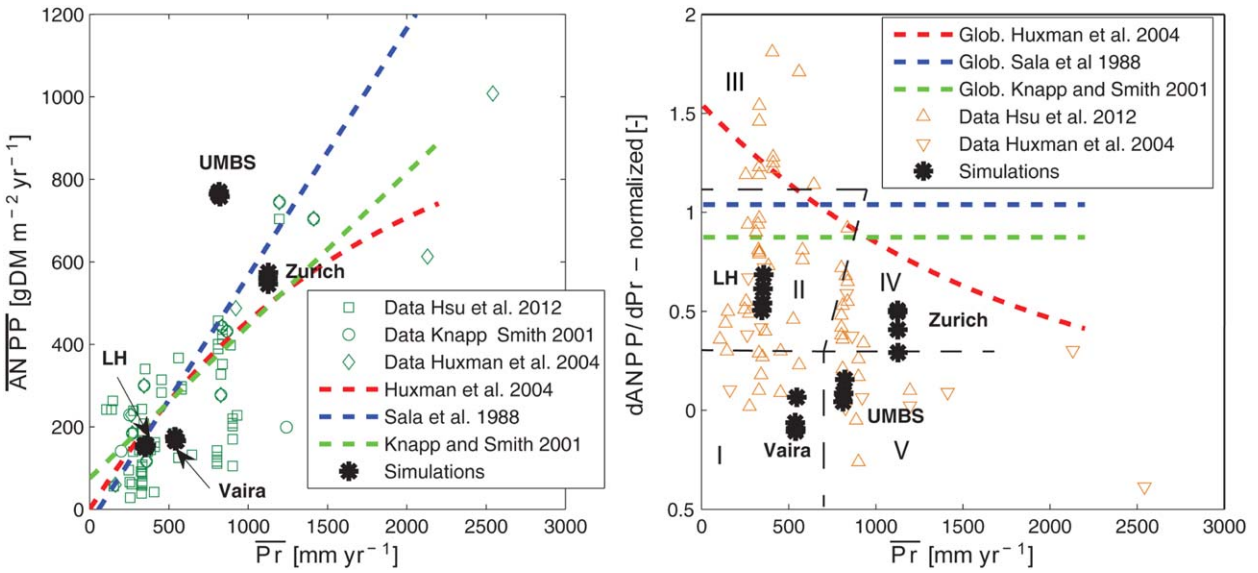

Figure 10. (a) Global-scale relationships [*Sala et al.*, 1988; *Knapp and Smith*, 2001; *Huxman et al.*, 2004] between the mean aboveground net primary production $\overline{ANPP}$ and mean precipitation $\overline{Pr}$, including empirical observations from *Knapp and Smith* [2001], *Huxman et al.* [2004], and *Hsu et al.* [2012] and model simulations carried out in this study (simulations). (b) Normalized local (single site) sensitivity of ANPP to changes in mean precipitation from the two databases of multiannual ANPP [*Huxman et al.*, 2004; *Hsu et al.*, 2012] and normalized sensitivity of multisite global-scale relationships compared with the model simulations carried out in this study (simulations).

As a consequence of previous results, deep leakage (Lk) or runoff are the most affected variables of the hydrological budget due to changes in precipitation interannual variability, as also expected from theoretical considerations [*Koster and Suarez*, 1999]. In this regard, we need to underline that all of the analyzed locations are not groundwater-dependent ecosystems. While a temporary water table may occur in the simulated soil columns, we do not explicitly simulate the effects of interannual variability in aquifers. Given the expected consequences of precipitation variability on deep leakage, it is likely that groundwater-fed ecosystems will experience a stronger sensitivity to changes in interannual variability [e.g., *Dunn et al.*, 2007] than found by our one-dimensional analysis, with no account for groundwater feedbacks.

4.2. Comparison With Global-Scale Relationships

In order to frame the study findings in a broader context, we compare our simulations with the global-scale relationship between $\overline{ANPP}$ and $\overline{Pr}$ (Figure 10a). Our results fit rather well for three out of the four locations. The productivity of UMBS is larger than expected from global-scale relationships but similar to other deciduous North American forests [*Knapp and Smith*, 2001; *Litton et al.*, 2007] and is well substantiated by empirical data [*Gough et al.*, 2008, 2009, 2013]. In addition, we report normalized local (single site) sensitivity for two global databases of multiannual ANPP [*Huxman et al.*, 2004; *Hsu et al.*, 2012] and compare these estimates with results of our simulations and the normalized sensitivity of multisite, global-scale relationships (Figure 10b). Our simulations are well within the variability obtained with empirical data at different sites worldwide. We suggest that at least five regions can be identified in the diagram of Figure 10b: (i) a region characterized by low-to-medium precipitation and low sensitivity, (ii) a region characterized by low-to-medium precipitation and intermediate sensitivity, (iii) a region characterized by low precipitation and high sensitivity, (iv) a region with medium-to-high precipitation and intermediate sensitivity, and (v) a region with medium-to-high precipitation and low sensitivity. The locations of the UMBS and Zürich tend to be represented by regions (iv) and (v), Vaira Ranch by region (i), and Lucky Hills by (ii). We note that for almost all of the locations, the local-scale sensitivity is significantly smaller than what would be expected from the multisite global-scale relationship. Only a few points in the region (iii) (corresponding to grasslands in Mongolia and Sevilleta, New Mexico) exhibit sensitivities stronger than the global-scale relationship. This result, while detected previously, although not in the present form, for vegetation productivity [*Lauenroth and Sala*, 1992; *Goward and Prince*, 1995; *Knapp and Smith*, 2001; *Huxman et al.*, 2004; *Hu et al.*, 2010] and also species

richness [*Cleland et al*., 2013], has important consequences in terms of predicting trajectories of changes using the computed sensitivities as a basis.

Specifically, it demonstrates that sensitivity of ecosystem productivity to a shift in precipitation at a given location can increase significantly, when the ecosystem has sufficient time and possibility to evolve from its current established condition to a new mature state. In other words, the time/space derivative of the global relationship reflecting a change in the vegetation composition and/or structure and/or form (i.e., either due to a transient evolution at a site or due to a "leap" in space) is much larger than the derivative obtained for a mature ecosystem in a dynamic steady state. This conclusion has important implications for interpretation of results obtained from manipulation studies lasting few years. Short experiments are likely to underestimate the sensitivity, if the ecosystem is in a dynamic steady state rather than in a transitional state [see also *Knapp et al*., 2012]. Note also that ecosystem shifts do not necessarily imply drastic ecosystem changes (e.g., from grassland to forest). Subtler changes in species composition or forest structure may also lead to new states with appreciable differences in water and carbon fluxes as demonstrated by factual observations [*Urbanski et al*., 2007; *Knapp et al*., 2012; *Hardiman et al*., 2013].

A similar analysis of local versus global sensitivities of evapotranspiration (ET) is relevant but hampered by the lack of independent annual ET observations. While computing long-term ET as precipitation less discharge is rather straightforward [*Roderick and Farquhar*, 2011; *Gentine et al*., 2012], the annual ET is more difficult to estimate because of the soil, groundwater, and snow storage effects. A possibility to overcome such a limitation is represented by direct measurement of latent heat flux from FLUXNET sites [*Baldocchi et al*., 2001; *Williams et al*., 2012]. However, the short record of observations available so far as well as the measurement issues [*Wilson et al*., 2002; *Leuning et al*., 2012] limit this possibility. Therefore, we use the Budyko relationship in the one-parameter form of *Fu* [1981] [see also *Zhang et al*., 2004] to infer global-scale sensitivities and compare them with the local-scale sensitivities computed in our simulations. The global-scale relationships of $\overline{ET}$ versus $\overline{Pr}$ depend on the Budyko's curve parameter ω and, most importantly, on the potential evapotranspiration (Table 1). The relationships are therefore different for each site (Figure 11). In order to account for the uncertainty in the ω parameter we used a wide range of $\omega=1.5-3.3$ [*Yang et al*., 2007; *Roderick and Farquhar*, 2011], which is roughly $\pm$35% of the reference value of 2.6 of the original Budyko's curve (Figure 11).

The normalized local sensitivities for the four analyzed locations are lower than the global sensitivity expected from Budyko's relationship, with two exceptions represented by the scenario ARp01 in Zürich and Lucky Hills (Figure 11). Although this result still requires local observations of annual ET to be properly validated, a conclusion similar to the one obtained for ANPP is proposed: ET sensitivity to changes in mean precipitation will considerably increase when the ecosystem undergoes a transition from a mature steady state toward a new equilibrium, with important consequences for long-term predictions of hydrological and energy fluxes.

The smaller sensitivity of the local-scale, as compared to the global-scale, relationships can be explained by the short-term controls of ET and GPP variability at the annual scale. These are mostly dictated by the repeated occurrence (or lack of thereof) of very favorable conditions within the year, e.g., "good hours." From our analysis, these controls appear to be primary contributors to annual fluxes in a mature established ecosystem. If a substantial species shift or a structural transition takes place, the sensitivity of ET and GPP to precipitation will increase until a new steady state is reached. This observation also has important implications in terms of predictability of changes. For short-term scales, predicting changes in the occurrence of "very favorable" conditions within a year is a more challenging task than predicting changes in seasonality or mean annual quantities. For long-term scales, changes in ET and GPP are more sensitive to changes in the mean climatic conditions but are mediated by shifts in ecosystem type and/or structure, which are also very difficult to predict. We remark that in combination to the noticeable importance of the short-term controls, we also found for all of the locations a dependence between the Horton index and the humidity index (supporting information, Figure S6), as suggested by previous literature. This underlines that the fraction of available water used as ET increases under drier conditions [*Troch et al*., 2009; *Brooks et al*., 2011].

4.3. Limits of Interpretation

We caution the reader that the presented results were obtained from numerical simulations and that the precipitation scenarios were designed to affect the ecohydrologic processes either through the linkages of

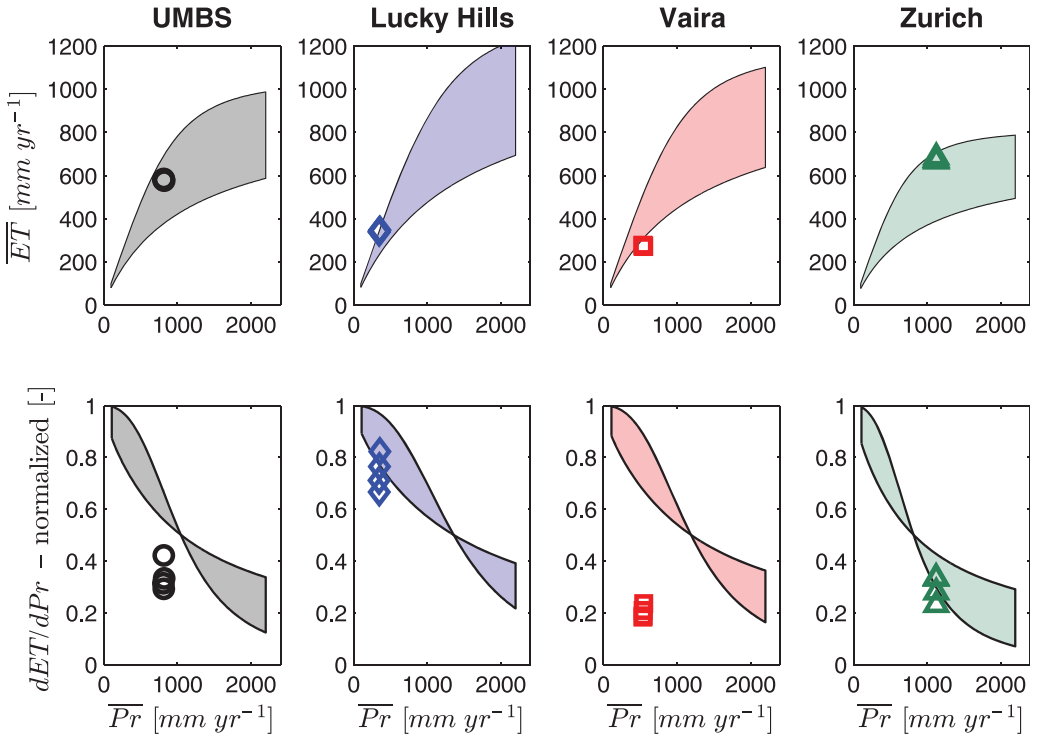

Figure 11. (top) Relationships between mean evapotranspiration $\overline{ET}$ and precipitation $\overline{Pr}$, as derived from the Budyko's curve in the one-parameter form [*Fu*, 1981], with the ω parameter assuming values in the range of ω=1.5−3.3. Since the curve depends on potential evapotranspiration, a different plot is obtained for each of the analyzed location. The simulated site-specific values are reported with the colored markers. (bottom) The normalized local sensitivity of evapotranspiration to changes in mean precipitation for the four analyzed locations from simulations (the colored markers) compared with the sensitivity obtained from the family of curves derived from the Budyko's relationship.

wetting regime with other meteorological variables (e.g., air temperature, humidity, radiation, etc.) or through the impacts on soil water availability. As results testify, the effects of the former are relatively minor; while there are more appreciable impacts of the latter for the driest (Lucky Hills) and grassland sites (Zürich), T-C incorporates a rather simple soil water stress control on stomatal dynamics [*Fatichi et al.*, 2012a]. Very severe or extreme droughts in addition to physiological (reversible) responses can lead to tree mortality because of hydraulic failure [*McDowell et al.*, 2011; *McDowell*, 2011; *Hoffmann et al.*, 2011] or drought-related infestation (e.g., pine beetles [*Clinton et al.*, 1993; *Kurz et al.*, 2008]), imposing structural and compositional (irreversible) changes [e.g., *Allen et al.*, 2010] and long-term carry-over effects in the system [e.g., *Leuzinger et al.*, 2005; *Blackman et al.*, 2009]. These effects are neglected or poorly simulated in T-C but have been shown to have important consequences on ecosystem carbon and water fluxes when ecosystems are strongly solicited by climate conditions [*Reichstein et al.*, 2002, 2007; *Granier et al.*, 2007]. Therefore, T-C likely overestimates ecosystem resilience to extreme droughts and interpretations are thus applicable to the mildly dry to wet range of water availabilities. However, extreme droughts can also trigger ecosystem shifts and thus support the notion of significantly higher sensitivities of global relationships that integrate space/time changes.

5. Conclusions

We simulated the response of four different ecosystems to four scenarios of interannual variability of precipitation using two advanced numerical tools, AWE-GEN and T-C, and a numerical experimentation approach. We found that sensitivities of ET and GPP to changes in the precipitation mean for specific locations and established ecosystems are 1–2 orders of magnitude larger than their sensitivities to changes in precipitation variance or long-memory of the process. As a result, an increase or decrease of the coefficient of variation of annual precipitation or an increase in its long-memory characteristics are mostly filtered and not

discernable in ET, T, and vegetation productivity but are expressed in variations of deep leakage and runoff. Short temporal scales, i.e., the occurrence of "good hours" was found to be the best explanatory variable for interannual variability of ET and ANPP for these ecosystems that were modeled to be in a dynamic steady state. As such, changes in precipitation interannual variability did not significantly affect the occurrence of "good hours," even though their frequency distribution starts being affected when soil control on water/carbon fluxes becomes progressively pronounced.

Local, single-site ET, and ANPP sensitivities to changes in precipitation mean are significantly smaller than sensitivities to precipitation gradients across climatic regions and vegetation communities, underlining a fundamental role of ecosystem reorganization through species shifts and/or structural modifications. These shifts might be also forced by extreme droughts, whose impacts are likely to be underestimated in this study because of the modeling assumptions. Fundamentally, the sensitivity of ET and ANPP to precipitation is altered and increased in the transitional stage, when an ecosystem undergoes reorganization (e.g., successional and invasion processes, shifts in composition). The results are obtained analyzing four ecosystems only but are well comprised within global relationships and are likely to be sufficiently general for other climates and vegetation types.

Acknowledgments

S.F. wishes to thank the organizers of the International Workshop on "Ecohydrology of semiarid environments: Confronting mathematical models with ecosystem complexity" held in May 2013 at Ben-Gurion University of the Negev, Israel, for stimulating this research. Authors are extremely grateful to all individuals involved in the collection of data and information at the FLUXNET sites that were used in the study. Meteorological data for Switzerland were provided by MeteoSwiss, the Federal Office of Meteorology and Climatology. V.Y.I. was partially supported by the NSF grant EAR 1151443 and the Visiting Faculty grant at the Institute of Environmental Engineering, ETH Zürich. All of the simulation results are available upon request to the authors.

References

Allen, C. D., et al. (2010), A global overview of drought and heat-induced tree mortality reveals emerging climate change risks for forests, *For. Ecol. Manage.*, *259*(4), 660–684.

Ammann, C., C. R. Flechard, J. Leifeld, A. Neftel, and J. Fuhrer (2007), The carbon budget of newly established temperate grassland depends on management intensity, *Agric., Ecosyst. Environ.*, *121*, 5–20.

Ammann, C., C. Spirig, J. Leifeld, and A. Neftel (2009), Assessment of the nitrogen and carbon budget of two managed temperate grassland fields, *Agric. Ecosyst. Environ.*, *133*, 150–162, doi:10.1016/j.agee.2009.05.006.

Baldocchi, D. (2008), Breathing of the terrestrial biosphere: Lessons learned from a global network of carbon dioxide flux measurement systems, *Aust. J. Bot.*, *56*, 1–26.

Baldocchi, D., et al. (2001), FLUXNET: A new tool to study the temporal and spatial variability of ecosystem-scale carbon dioxide, water vapor, and energy flux densities, *Bull. Am. Meteorol. Soc.*, *82*(11), 2415–2434.

Baldocchi, D. D., L. Xu, and N. Kiang (2004), How plant functional-type, weather, seasonal drought, and soil physical properties alter water and energy fluxes of an oak-grass savanna and an annual grassland, *Agric. For. Meteorol.*, *123*, 13–39, doi:10.1016/j.agrformet.2003.11.006.

Beran, J. (1994), *Statistic for Long-Memory Processes*, Chapman and Hall, New York.

Blackman, C. J., T. J. Brodribb, and G. J. Jordan (2009), Leaf hydraulics and drought stress: Response, recovery and survivorship in four woody temperate plant species, *Plant Cell Environ.*, *32*, 1584–1595.

Bonan, G. B. (2008), Forests and climate change: Forcings, feedbacks, and the climate benefits of forests, *Science*, *320*, 1444–1449, doi:10.1126/science.1155121.

Bovard, B. D., P. S. Curtis, C. S. Vogel, H.-B. Su, and H. P. Schmid (2005), Environmental controls on sap flow in a northern hardwood forest, *Tree Physiol.*, *25*, 31–38.

Bréda, N., R. Huc, A. Granier, and E. Dreyer (2006), Temperate forest trees and stands under severe drought: A review of ecophysiological responses, adaptation processes and long-term consequence, *Ann. For. Sci.*, *63*, 625–644, doi:10.1051/forest:2006042.

Brooks, P. D., P. A. Troch, M. Durcik, E. Gallo, and M. Schlegel (2011), Quantifying regional scale ecosystem response to changes in precipitation: Not all rain is created equal, *Water Resour. Res.*, *47*, W00J08, doi:10.1029/2010WR009762.

Cleland, E. E., et al. (2013), Sensitivity of grassland plant community composition to spatial vs. temporal variation in precipitation, *Ecology*, *94*(8), 1687–1696.

Clinton, B. D., L. R. Boring, and W. T. Swank (1993), Canopy gap characteristics and drought influences in oak forests of the Coweeta basin, *Ecology*, *74*, 1551–1558.

Collins, S. L., S. E. K. J. A. Plaut, J. G. Okie, D. Brese, L. B. Calabrese, A. Carvajal, R. J. Evansen, and E. Nonaka (2012), Stability of tallgrass prairie during a 19-year increase in growing season precipitation, *Funct. Ecol.*, *26*, 1450–1459, doi:10.1111/j.1365-2435.2012.01995.x.

Cox, J. R., G. W. Fraiser, and K. G. Renard (1986), Biomass distribution at grassland and shrubland sites, *Rangelands*, *8*(2), 67–69.

Curtis, P. S., C. S. Vogel, C. M. Gough, H. P. Schmid, H. B. Su, and B. D. Bovard (2005), Respiratory carbon losses and the carbon-use efficiency of a northern hardwood forest, 1999–2003, *New Phytol.*, *167*(2), 437–455.

D'Odorico, P., and A. Bhattachan (2012), Hydrologic variability in dryland regions: Impacts on ecosystem dynamics and food security, *Philos. Trans. R. Soc. B*, *367*, 3145–3157.

Dunn, A. L., C. C. Barford, S. C. Wofsy, M. L. Goulden, and B. C. Daube (2007), A long-term record of carbon exchange in a boreal black spruce forest: Means, responses to interannual variability, and decadal trends, *Global Change Biol.*, *13*, 577–590, doi:10.1111/j.1365-2486.2006.01221.x.

Emmerich, W. E., and C. L. Verdugo (2008), Long-term carbon dioxide and water flux database, Walnut Gulch Experimental Watershed, Arizona, United States, *Water Resour. Res.*, *44*, W05S09, doi:10.1029/2006WR005693.

Fang, J. Y., S. L. Piao, Z. Y. Tang, C. H. Peng, and W. Ji (2001), Interannual variability in net primary production and precipitation, *Science*, *293*, 1723.

Fatichi, S. (2010), *The modeling of hydrological cycle and its interaction with vegetation in the framework of climate change*, PhD thesis, Univ. of Firenze, Firenze, Italy.

Fatichi, S., and S. Leuzinger (2013), Reconciling observations with modeling: The fate of water and carbon allocation in a mature deciduous forest exposed to elevated CO_2, *Agric. For. Meteorol.*, *174–175*, 144–157, doi:10.1016/j.agrformet.2013.02.005.

Fatichi, S., V. Y. Ivanov, and E. Caporali (2011), Simulation of future climate scenarios with a weather generator, *Adv. Water Resour.*, *34*, 448–467, doi:10.1016/j.advwatres.2010.12.013.

Fatichi, S., V. Y. Ivanov, and E. Caporali (2012a), A mechanistic ecohydrological model to investigate complex interactions in cold and warm water-controlled environments: 1. Theoretical framework and plot-scale analysis, *J. Adv. Model. Earth Syst.*, *4*, M05002, doi:10.1029/2011MS000086.

Fatichi, S., V. Y. Ivanov, and E. Caporali (2012b), A mechanistic ecohydrological model to investigate complex interactions in cold and warm water-controlled environments: 2. Spatiotemporal analyses, *J. Adv. Model. Earth Syst.*, *4*, M05003, doi:10.1029/2011MS000087.

Fatichi, S., V. Y. Ivanov, and E. Caporali (2012c), Investigating interannual variability of precipitation at the global scale: Is there a connection with seasonality?, *J. Clim.*, *25*(16), 5512–5523, doi:10.1175/JCLI-D-11-00356.1.

Fatichi, S., V. Y. Ivanov, and E. Caporali (2013), Assessment of a stochastic downscaling methodology in generating an ensemble of hourly future climate time series, *Clim. Dyn.*, *40*(7–8), 1841–1861, doi:10.1007/s00382-012-1627-2.

Fatichi, S., M. J. Zeeman, J. Fuhrer, and P. Burlando (2014), Ecohydrological effects of management on subalpine grasslands: From local to catchment scale, *Water Resour. Res.*, *50*, 148–164, doi:10.1002/2013WR014535.

Fu, B. P. (1981), On the calculation of the evaporation from land surface [in Chinese], *Sci. Atmos. Sin.*, *5*(1), 23–31.

Gentine, P., P. D'Odorico, B. R. Lintner, G. Sivandran, and G. Salvucci (2012), Interdependence of climate, soil, and vegetation as constrained by the Budyko curve, *Geophys. Res. Lett.*, *39*, L19404, doi:10.1029/2012GL053492.

Gilgen, A. K. (2009), *Drought in Swiss grasslands at different altitudes: Effects on productivity and resource use*, PhD thesis, ETH Zurich, Zurich, Switzerland.

Gilgen, A. K., and N. Buchmann (2009), Response of temperate grasslands at different altitudes to simulated summer drought differed but scaled with annual precipitation, *Biogeosciences*, *6*, 2525–2539.

Gough, C. M., C. S. Vogel, C. Kazanski, L. Nagel, C. E. Flower, and P. S. Curtis (2007), Coarse-woody debris and the carbon balance of a north temperate forest, *For. Ecol. Manage.*, *244*(1–3), 60–67.

Gough, C. M., C. S. Vogel, H. P. Schmid, and P. S. Curtis (2008), Controls on annual forest carbon storage: Lessons from the past and predictions for the future, *BioScience*, *58*(7), 609–622.

Gough, C. M., C. E. Flower, C. S. Vogel, D. Dragoni, and P. S. Curtis (2009), Whole-ecosystem labile carbon production in a north temperate deciduous forest, *Agric. For. Meteorol.*, *149*, 1531–1540, doi:10.1016/j.agrformet.2009.04.006.

Gough, C. M., B. S. Hardiman, L. E. Nave, G. Bohrer, K. D. Maurer, C. S. Vogel, K. J. Nadelhoffer, and P. S. Curtis (2013), Sustained carbon uptake and storage following moderate disturbance in a great lakes forest, *Ecol. Appl.*, *23*(5), 1202–1215.

Goward, S. N., and S. D. Prince (1995), Transient effects of climate on vegetation dynamics: Satellite observations, *J. Biogeogr.*, *22*(2/3), 549–564.

Granier, A., et al. (2007), Evidence for soil water control on carbon and water dynamics in European forests during the extremely dry year: 2003, *Agric. For. Meteorol.*, *143*, 123–145.

Guo, Q., Z. Hu, S. Li, X. Li, X. Sun, and G. Yu (2012), Spatial variations in aboveground net primary productivity along a climate gradient in Eurasian temperate grassland: Effects of mean annual precipitation and its seasonal distribution, *Global Change Biol.*, *18*, 3624–3631, doi:10.1111/gcb.12010.

Hardiman, B. S., C. M. Gough, A. Halperin, K. L. Hofmeister, L. E. Nave, G. Bohrer, and P. S. Curtis (2013), Maintaining high rates of carbon storage in old forests: A mechanism linking canopy structure to forest function, *For. Ecol. Manage.*, *298*, 111–119.

He, L., V. Y. Ivanov, G. Bohrer, J. E. Thomsen, C. S. Vogel, and M. Moghaddam (2013), Temporal dynamics of soil moisture in a northern temperate mixed successional forest after a prescribed intermediate disturbance, *Agric. For. Meteorol.*, *180*, 22–33, doi:10.1016/j.agrformet.2013.04.014.

He, L., V. Y. Ivanov, G. Bohrer, K. D. Maurer, C. S. Vogel, and M. Moghaddam (2014), Effects of fine-scale soil moisture and canopy heterogeneity on energy and water fluxes in a northern temperate mixed forest, *Agric. For. Meteorol.*, *184*, 243–256, doi:10.1016/j.agrformet.2013.10.006.

Hoffmann, W. A., R. M. Marchin, P. Abit, and O. L. Lau (2011), Hydraulic failure and tree dieback are associated with high wood density in a temperate forest under extreme drought, *Global Change Biol.*, *17*, 2731–2742.

Holmgren, M., M. Hirota, E. H. van Nes, and M. Scheffer (2013), Effects of interannual climate variability on tropical tree cover, *Nat. Clim. Change*, *3*, 755–758, doi:10.1038/nclimate1906.

Hsu, J. S., J. Powell, and P. B. Adler (2012), Sensitivity of mean annual primary production to precipitation, *Global Change Biol.*, *18*, 2246–2255, doi:10.1111/j.1365–2486.2012.02687.x.

Hu, Z., Y. Guirui, F. Jiangwen, Z. Huaping, W. Shaoqiang, and L. Shenggong (2010), Precipitation-use efficiency along a 4500-km grassland transect, *Global Ecol. Biogeogr.*, *19*, 842–851.

Huxman, T. E., et al. (2004), Convergence across biomes to a common rain use efficiency, *Nature*, *429*, 651–654.

Ivanov, V. Y., R. L. Bras, and D. C. Curtis (2007), A weather generator for hydrological, ecological, and agricultural applications, *Water Resour. Res.*, *43*, W10406, doi:10.1029/2006WR005364.

Jensen, J. (1906), On the convex functions and inequalities between mean values, *Acta Math.*, *30*, 175–193.

Keefer, T. O., M. S. Moran, and G. B. Paige (2008), Long-term meteorological and soil hydrology database, Walnut Gulch Experimental Watershed, Arizona, United States, *Water Resour. Res.*, *44*, W05S07, doi:10.1029/2006WR005702.

King, D. M., S. M. Skirvin, C. H. Collins, M. S. Moran, S. H. Biedenbender, M. R. Kidwell, M. A. Weltz, and A. Diaz-Gutierrez (2008), Assessing vegetation change temporally and spatially in southeastern Arizona, *Water Resour. Res.*, *44*, W05S15, doi:10.1029/2006WR005850.

Knapp, A. K., and M. D. Smith (2001), Variation among biomes in temporal dynamics of aboveground primary production, *Science*, *291*, 481–484.

Knapp, A. K., J. M. Briggs, and J. K. Koelliker (2001), Frequency and extent of water limitation to primary production in a mesic temperate grassland, *Ecosystems*, *4*, 19–28.

Knapp, A. K., J. M. Briggs, and M. D. Smith (2012), Community stability does not preclude ecosystem sensitivity to chronic resource alteration, *Funct. Ecol.*, *26*, 1231–1233, doi:10.1111/j.1365-2435.2012.02053.x.

Koster, R. D., and M. J. Suarez (1999), A simple framework for examining the interannual variability of land surface moisture fluxes, *J. Clim.*, *12*, 1911–1917.

Koutsoyiannis, D. (2003), Climate change, the Hurst phenomenon and hydrological statistics, *Hydrol. Sci. J.*, *48*(1), 3–24.

Kurz, W. A., C. C. Dymond, G. Stinson, G. J. Rampley, E. T. Neilson, A. L. Carroll, T. Ebata, and L. Safranyik (2008), Mountain pine beetle and forest carbon feedback to climate change, *Nature*, *452*, 987–990.

Lauenroth, W. K., and O. E. Sala (1992), Long-term forage production of North-American shortgrass steppe, *Ecol. Appl.*, *2*, 397–403.

Lazzarotto, P., P. Calanca, and J. Fuhrer (2009), Dynamics of grassclover mixtures—An analysis of the response to management with the PROductive GRASsland Simulator (PROGRASS), *Ecol. Model.*, *220*, 703–724.

Leuning, R., E. van Gorsel, W. J. Massman, and P. R. Isaac (2012), Reflections on the surface energy imbalance problem, *Agric. For. Meteorol.*, *156*, 65–74, doi:10.1016/j.agrformet.2011.12.002.
Leuzinger, S., G. Zotz, R. Asshoff, and C. Körner (2005), Responses of deciduous forest trees to severe drought in Central Europe, *Tree Physiol.*, *25*, 641–650.
Litton, C. M., J. W. Raich, and M. G. Ryan (2007), Carbon allocation in forest ecosystems, *Global Change Biol.*, *13*, 2089–2109, doi:10.1111/j.1365-2486.2007.01420.x.
Ma, S., D. D. Baldocchi, L. Xu, and T. Hehn (2007), Inter-annual variability in carbon dioxide exchange of an oak/grass savanna and open grassland in California, *Agric. For. Meteorol.*, *147*, 157–171, doi:10.1016/j.agrformet.2007.07.008.
McDowell, N. G. (2011), Mechanisms linking drought, hydraulics, carbon metabolism, and mortality, *Plant Physiol.*, *155*, 1051–1059.
McDowell, N. G., D. J. Beerling, D. D. Breshears, R. A. Fisher, K. F. Raffa, and M. Stitt (2011), The interdependent mechanisms underlying climate-driven vegetation mortality, *Trends Ecol. Evol.*, *26*(10), 523–532.
Medlyn, B. E., A. P. Robinson, R. Clement, and R. E. McMurtrie (2005), On the validation of models of forest CO_2 exchange using eddy covariance data: Some perils and pitfalls, *Tree Physiol.*, *25*(7), 839–857.
Montanari, A., R. Rosso, and M. S. Taqqu (1997), Fractionally differenced ARIMA models applied to hydrologic time series: Identification, estimation and simulation, *Water Resour. Res.*, *33*(5), 1035–1044.
Oishi, A. C., R. Oren, K. A. Novick, S. Palmroth, and G. G. Katul (2010), Interannual invariability of forest evapotranspiration and its consequence to water flow downstream, *Ecosystems*, *13*, 421–436, doi:10.1007/s10021-010-9328-3.
Oren, R., et al. (2001), Soil fertility limits carbon sequestration by forest ecosystems in a CO_2-enriched atmosphere, *Nature*, *411*, 469–472.
Phillips, N., and R. Oren (2001), Intra- and inter-annual variation in transpiration of a pine forest, *Ecol. Appl.*, *11*(2), 385–396.
Reichstein, M., J. D. Tenhunen, O. Roupsard, J.-M. Ourcival, S. Rambal, F. Miglietta, A. Peressotti, M. Pecchiari, G. Tirone, and R. Valentini (2002), Severe drought effects on ecosystem CO_2 and H_2O fluxes at three Mediterranean evergreen sites: Revision of current hypotheses?, *Global Change Biol.*, *8*, 999–1017, doi:10.1046/j.1365-2486.2002.00530.x.
Reichstein, M., et al. (2007), Reduction of ecosystem productivity and respiration during the European summer 2003 climate anomaly: A joint flux tower, remote sensing and modelling analysis, *Global Change Biol.*, *13*, 634–651, doi:10.1111/j.1365-2486.2006.01224.x.
Roberts, J. (1983), Forest transpiration: A conservative hydrological process?, *J. Hydrol.*, *66*, 133–141.
Roderick, M. L., and G. D. Farquhar (2011), A simple framework for relating variations in runoff to variations in climatic conditions and catchment properties, *Water Resour. Res.*, *47*, W00G07, doi:10.1029/2010WR009826.
Rowell, D. P. (2005), A scenario of European climate change for the late twenty-first century: Seasonal means and interannual variability, *Clim. Dyn.*, *25*, 837–849, doi:10.1007/s00382-005-0068-6.
Ryu, Y., D. D. Baldocchi, S. Ma, and T. Hehn (2008), Interannual variability of evapotranspiration and energy exchange over an annual grassland in California, *J. Geophys. Res.*, *113*, D09104, doi:10.1029/2007JD009263.
Sala, O. E., W. J. Parton, L. A. Joyce, and W. K. Lauenroth (1988), Primary production of the central grassland region of the United States, *Ecology*, *69*, 40–45.
Schmid, H. P., C. S. B. Grimmond, F. Cropley, B. Offerle, and H. B. Su (2000), Measurements of CO_2 and energy fluxes over a mixed hardwood forest in the mid-western United States, *Agric. For. Meteorol.*, *103*(4), 357–374.
Sellers, P. J., et al. (1997), Modeling the exchanges of energy, water and carbon between continents and the atmosphere, *Science*, *275*, 502–509.
Shuttleworth, W. J. (1993), Evaporation, in *Handbook of Hydrology*, pp. 4.1–4.53, McGraw-Hill, New York.
Skirvin, S., M. Kidwell, S. Biedenbender, J. P. Henley, D. King, C. H. Collins, S. Moran, and M. Weltz (2008), Vegetation data, Walnut Gulch Experimental Watershed, Arizona, United States, *Water Resour. Res.*, *44*, W05S08, doi:10.1029/2006WR005724.
Stoy, P. C., G. G. Katul, M. B. S. Siqueira, J.-Y. Juang, K. A. Novick, H. R. McCarthy, A. C. Oishi, J. M. Uebelherr, H.-S. Kim, and R. Oren (2006), Separating the effects of climate and vegetation on evapotranspiration along a successional chronosequence in the southeastern US, *Global Change Biol.*, *12*, 1–21, doi:10.1111/j.1365-2486.2006.01244.x.
Su, H. B., H. P. Schmid, C. S. B. Grimmond, C. S. Vogel, and A. J. Oliphant (2004), Spectral characteristics and correction of long-term eddy-covariance measurements over two mixed hardwood forests in non-flat terrain, *Boundary Layer Meteorol.*, *110*(2), 213–253.
Troch, P. A., G. F. Martinez, V. R. N. Pauwels, M. Durcik, M. Sivapalan, C. Harman, P. D. Brooks, H. Gupta, and T. Huxman (2009), Climate and vegetation water use efficiency at catchment scales, *Hydrol. Processes*, *23*, 2409–2414, doi:10.1002/hyp.7358.
Urbanski, S., C. Barford, S. Wofsy, C. Kucharik, E. Pyle, J. Budney, K. McKain, D. Fitzjarrald, M. Czikowsky, and J. W. Munger (2007), Factors controlling CO_2 exchange on timescales from hourly to decadal at Harvard Forest, *J. Geophys. Res.*, *112*, G02020, doi:10.1029/2006JG000293.
Weltz, M. A., J. C. Ritchie, and H. D. Fox (1994), Comparison of laser and field measurements of vegetation height and canopy cover, *Water Resour. Res.*, *30*(5), 1311–1319.
Williams, C. A., and J. D. Albertson (2005), Contrasting short- and long-timescale effects of vegetation dynamics on water and carbon fluxes in water-limited ecosystems, *Water Resour. Res.*, *41*, W06005, doi:10.1029/2004WR003750.
Williams, C. A., et al. (2012), Climate and vegetation controls on the surface water balance: Synthesis of evapotranspiration measured across a global network of flux towers, *Water Resour. Res.*, *48*, W06523, doi:10.1029/2011WR011586.
Wilson, K., et al. (2002), Energy balance closure at FLUXNET sites, *Agric. For. Meteorol.*, *113*, 223–243.
Wilson, K. B., and D. D. Baldocchi (2000), Seasonal and interannual variability of energy fluxes over a broadleaved temperate deciduous forest in North America, *Agric. For. Meteorol.*, *100*, 1–18.
Xu, L., and D. D. Baldocchi (2004), Seasonal variation in carbon dioxide exchange over a Mediterranean annual grassland in California, *Agric. For. Meteorol.*, *1232*, 79–96, doi:10.1016/j.agrformet.2003.10.004.
Yang, D., F. Sun, Z. Liu, Z. Cong, G. Ni, and Z. Lei (2007), Analyzing spatial and temporal variability of annual water-energy balance in nonhumid regions of China using the Budyko hypothesis, *Water Resour. Res.*, *43*, W04426, doi:10.1029/2006WR005224.
Yang, Y., J. Fang, W. Ma, and W. Wan (2008), Relationship between variability in aboveground net primary production and precipitation in global grasslands, *Geophys. Res. Lett.*, *35*, L23710, doi:10.1029/2008GL035408.
Zeeman, M. J., R. Hiller, A. K. Gilgen, P. Michna, P. Plüss, N. Buchmann, and W. Eugster (2010), Management and climate impacts on net CO_2 fluxes and carbon budgets of three grasslands along an elevational gradient in Switzerland, *Agric. For. Meteorol.*, *150*, 519–530, doi:10.1016/j.agrformet.2010.01.011.
Zhang, L., K. Hickel, W. R. Dawes, F. H. S. Chiew, A. W. Western, and P. R. Briggs (2004), A rational function approach for estimating mean annual evapotranspiration, *Water Resour. Res.*, *40*, W02502, doi:10.1029/2003WR002710.